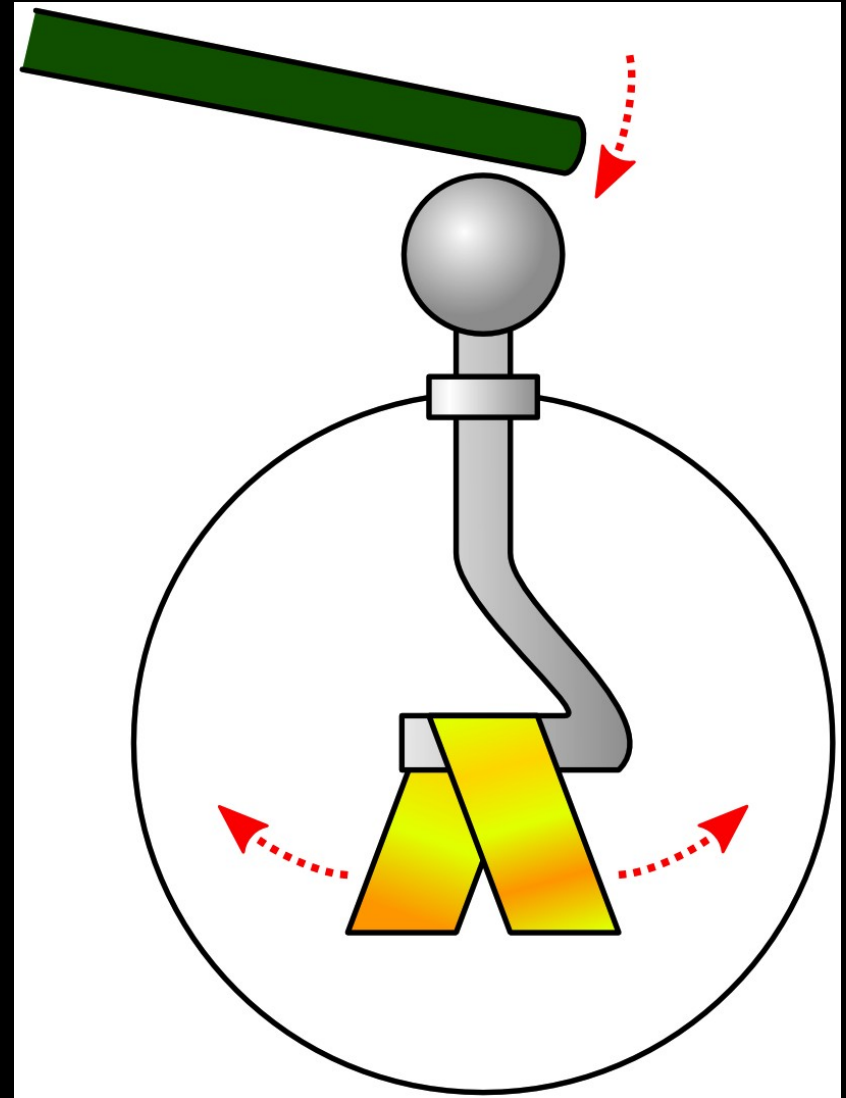


The discovery of Cosmic Rays

at the beginning of the 20th century, the discharge rate of an electroscope was used as a measure of the level of radioactivity

electroscopes discharge slowly even in the absence of a radioactive source -> background radiation

radiation from radioactive materials in the Earth?



ELECTROSCOPE



LA RADIAZIONE PENETRANTE ALLA SUPERFICIE ED IN SENO ALLE ACQUE.

NOTA DI D. PACINI.

Nelle acque marine di Livorno e in quelle del lago di Bracciano fra giugno e ottobre 1911 registro' la diminuzione dell'intensità all'aumentare della profondità

*“Esiste nell'atmosfera una sensibile causa ionizzante,
con radiazioni penetranti,
indipendente dall'azione diretta delle sostanze radioattive del terreno.”*

The discovery of Cosmic Rays

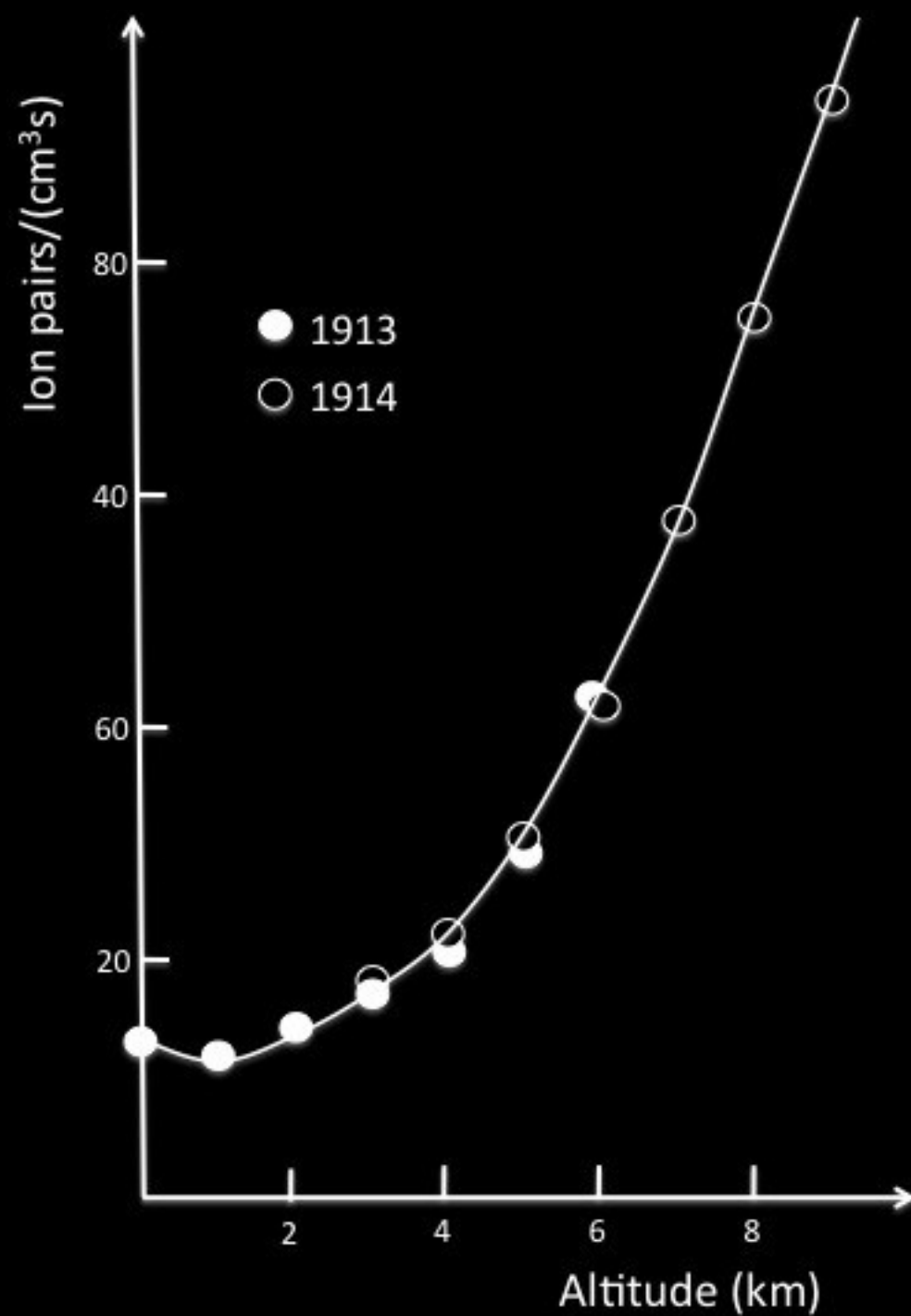
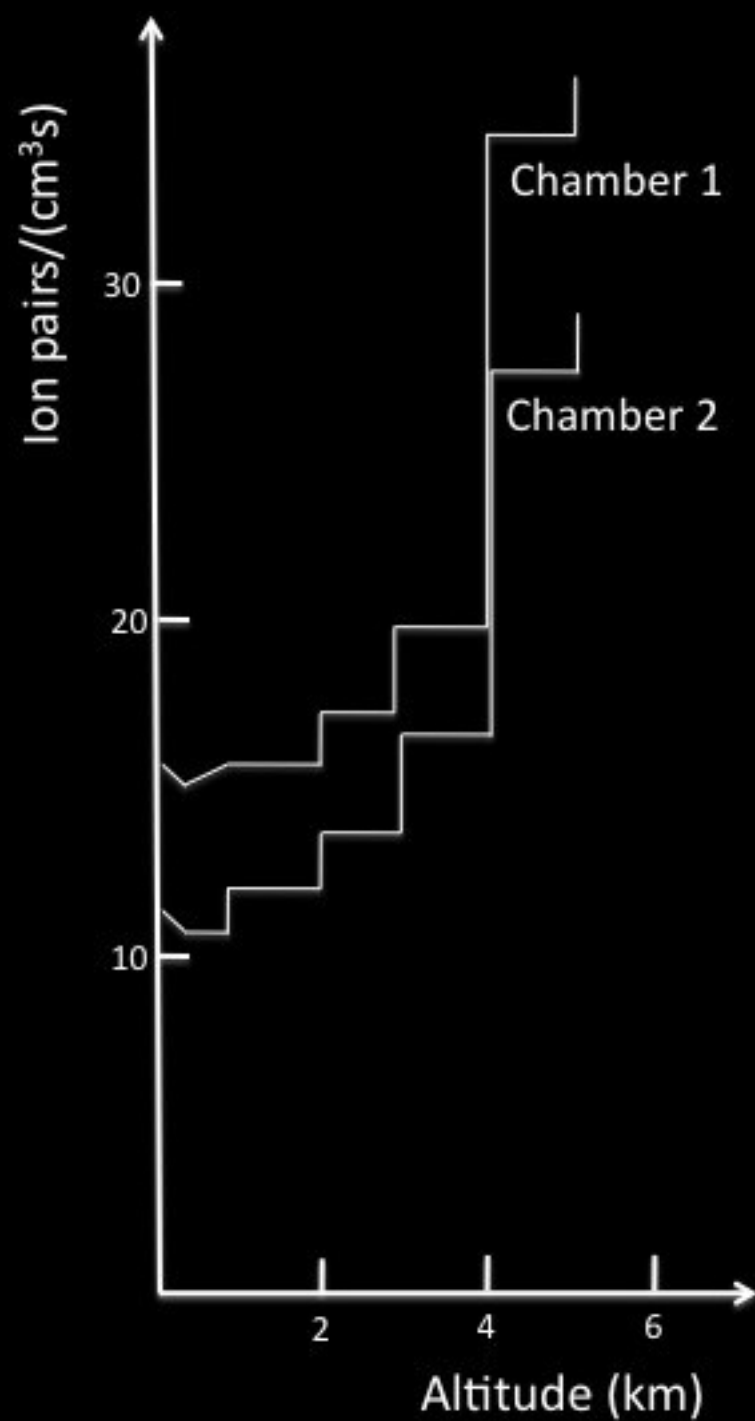
If due to radioactive materials in the Earth, the effect should diminish with height

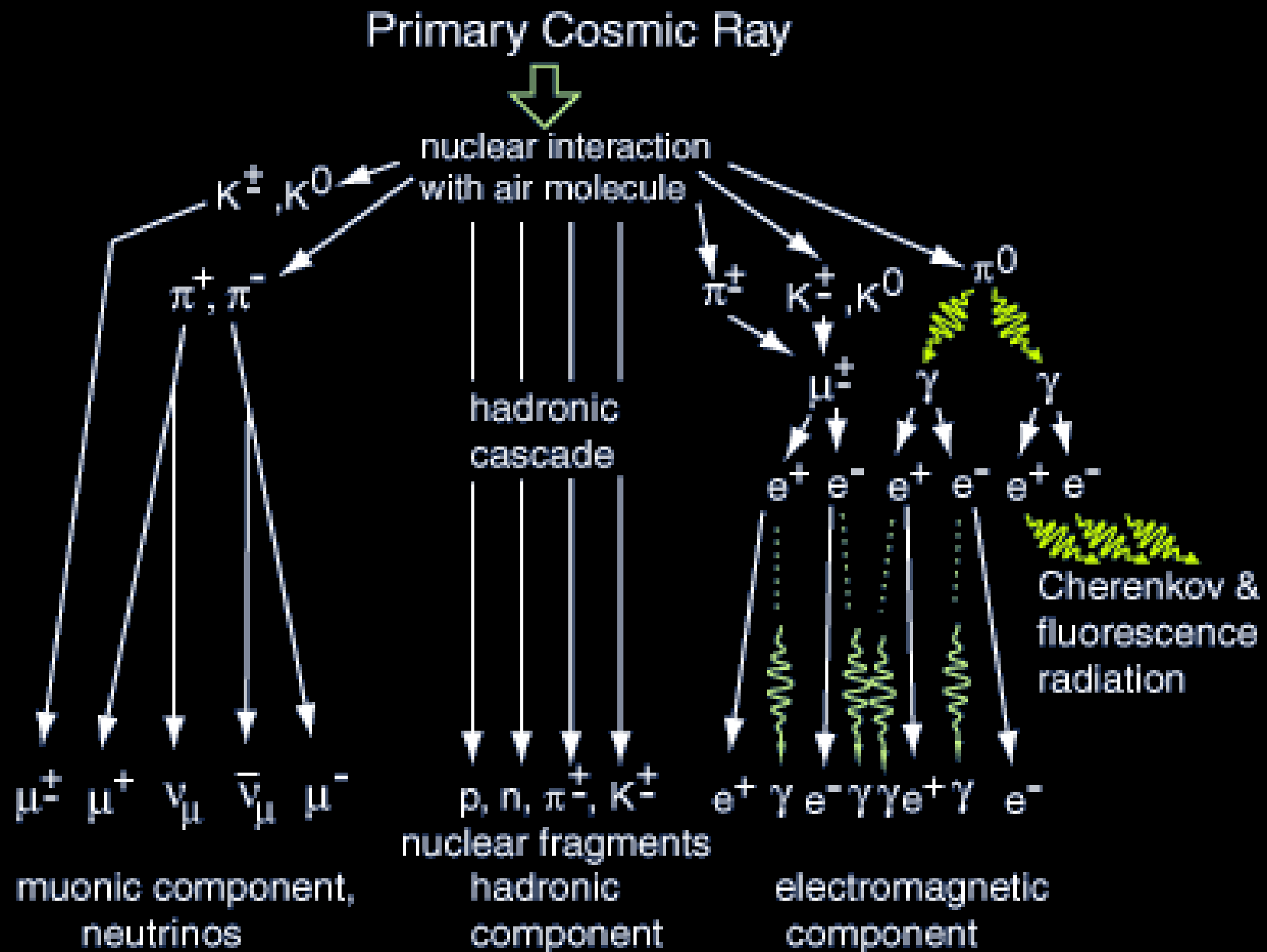
In 1912, during a balloon flight Victor Hess discovered that the effect was indeed **increasing with height**, and concluded that:

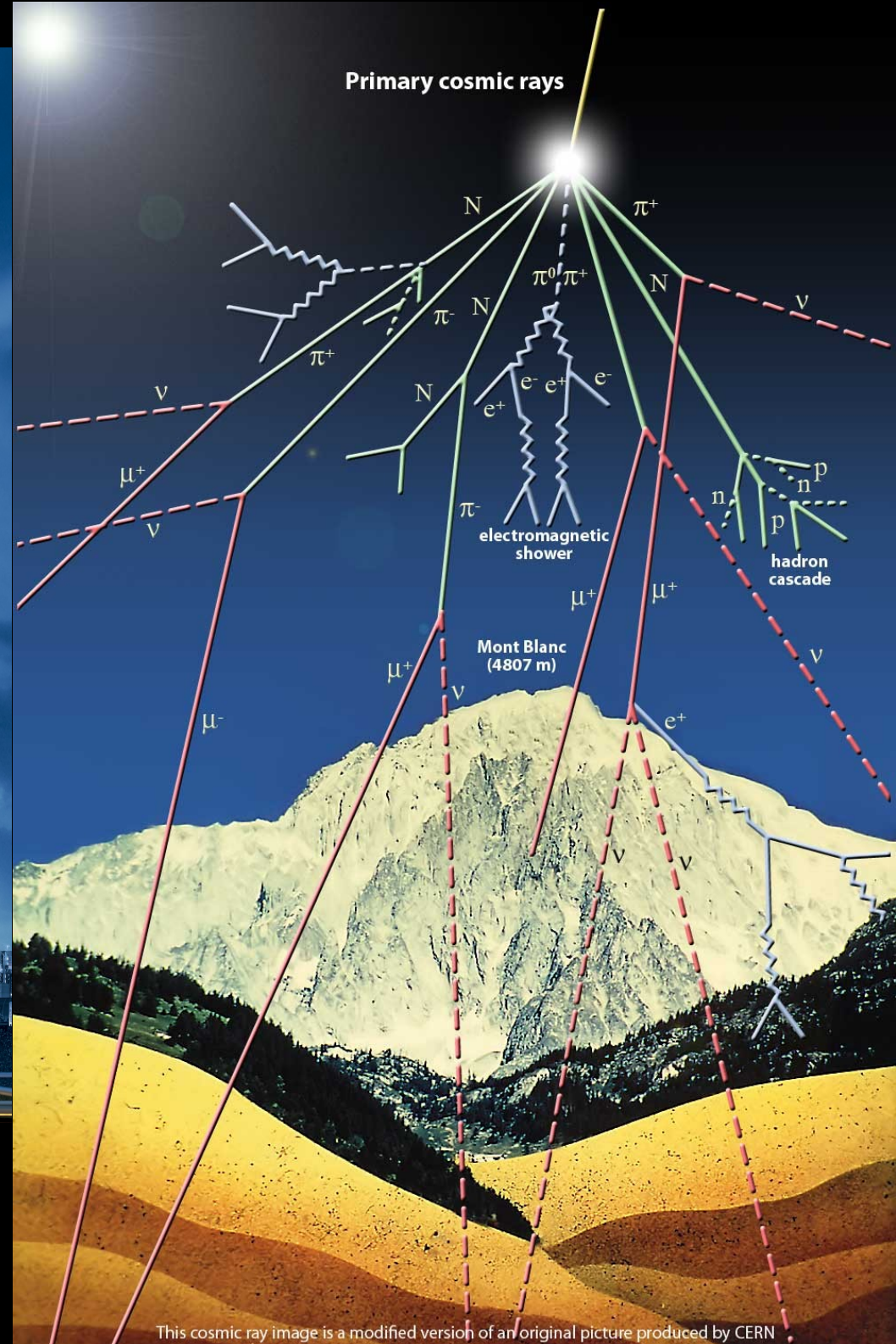
“a radiation of very high penetrating power enters our atmosphere from above”



V. Hess in 1912







This cosmic ray image is a modified version of an original picture produced by CERN

What are Cosmic Rays?

- Cosmic rays particles hit the Earth's atmosphere at the rate of about **1000 per square meter per second**.
- They are ionized nuclei - about **90% protons**, 9% alpha particles and the rest heavy nuclei - and they are distinguished by their high energies.
- Most cosmic rays are **relativistic**, having energies comparable or somewhat greater than their masses.
 - A very few of them have ultrarelativistic energies extending up to 10^{20} eV (about 20 Joules), eleven order of magnitudes greater than the equivalent rest mass energy of a proton.

The fundamental question of cosmic ray physics is,

“Where do they come from?”

and in particular,

“How are they accelerated to such high energies?”.

Instrument	Species	Energy per nucleon	Reference
Nuclei			
PAMELA	p, He	100 MeV–1 TeV	Adriani et al. 2011; 2013a,b
AMS-02	p	1 GeV–1.8 TeV	Consolandi et al. 2014
AMS-02	He	2 GeV–3 TeV	Choutko et al. 2013
ACE	Isotopes B–Ni	few 100 MeV	Lave et al. 2013
AMS-01	Isotopes of H, He, Li, Be, B	0.2–1.4 GeV	Aguilar et al. 2011 and references therein
PAMELA	Isotopes of p, He	100–900 MeV	Adriani et al. 2013c
ATIC-2	p, He, C, O, Ne, Mg, Si, Fe	50 GeV–200 TeV	Panov et al. 2009
PAMELA	B/C	0.44–129 GeV	Adriani et al. 2014
AMS-02	B/C	0.5–700 GeV	Oliva et al. 2013
PAMELA	d	50–650 MeV	Koldobskiy et al. 2013
CREAM	C–Fe	500 GeV–few TeV	Ahn et al. 2008, 2009, 2010; Yoon et al. 2011
TRACER	B–Fe, B/C	1 GeV–1 TeV	Obermeier et al. 2011
TIGER	Elements Fe–Se	0.35–250 GeV	Rauch et al. 2009
PAMELA	p	60 MeV–350 GeV	Mayorov et al. 2013
BESS-Polar	p	170 MeV–3.5 GeV	Abe et al. 2012
Leptons			
ATIC-1,2	e^- , e^+	20 GeV–2.3 TeV	Chang et al. 2008
HESS	$e^- + e^+$	340 GeV–3 TeV	Aharonian et al. 2008, 2009
<i>Fermi</i> -LAT	$e^- + e^+$	7 GeV–1 TeV	Ackermann et al. 2010
<i>Fermi</i> -LAT	e^- , e^+	20–200 GeV	Ackermann et al. 2012f
PAMELA	e^- , e^+	1–300 GeV	Adriani et al. 2009, 2013d; Mikhailov et al. 2013
AMS-02	e^- , e^+	0.5–700 GeV	Aguilar et al. 2013, Battiston 2014

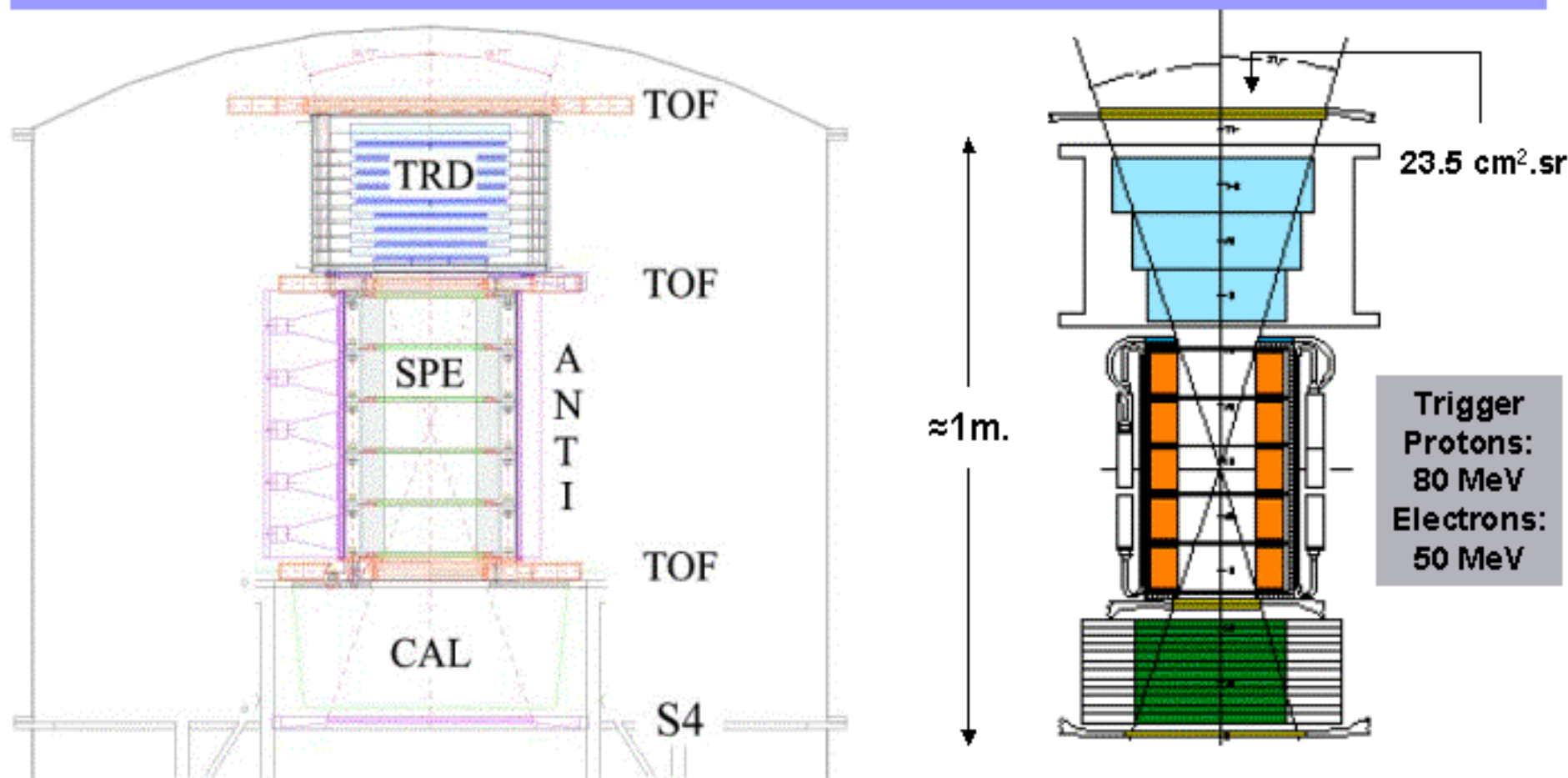
PAMELA

Payload for Antimatter/Matter Exploration and Light-nuclei Astrophysics

- Direct detection of CRs in space
- Main focus on antimatter component



The Pamela telescope concept (1)



TRD: Transition Radiation Detector to identify **electron and positron** ($>1 \text{ GeV}$).

Permanent Magnet: equipped with **silicon tracker** ($B=0.4 \text{ tesla}$, spatial res. $=7 \mu\text{m}$).

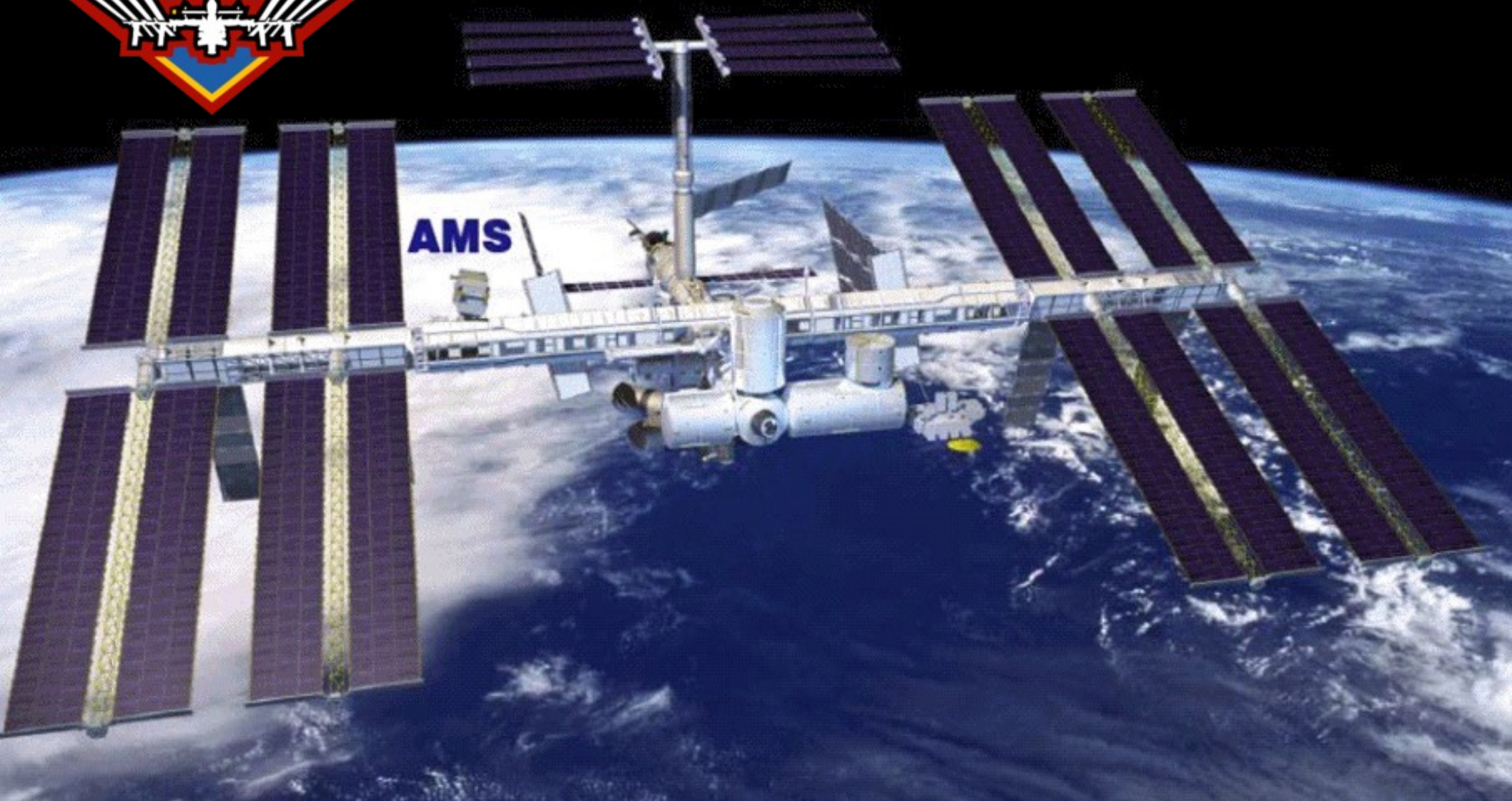
Imaging Calorimeter: silicon detector and tungsten absorber (pitch $=3.6 \text{ mm}$., $16 X_0$, $0.9 \lambda_i$).

TOF and Trigger counters: 3 planes (5 layers). Resolution $=150 \text{ ps}$. e/p rejection below 1 GeV .

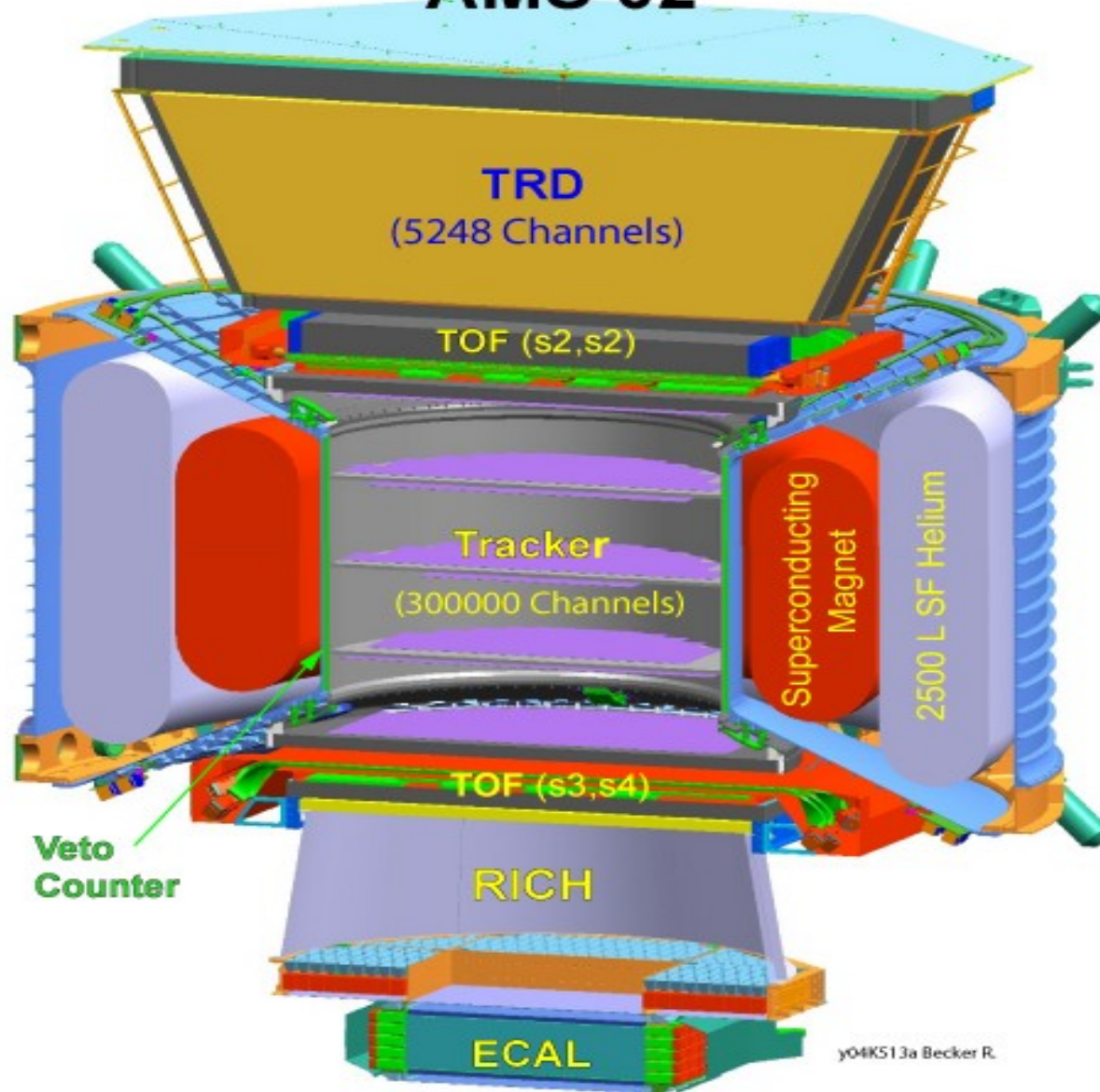
Anticoincidence counters: geometrical definition and particle showering shielding.

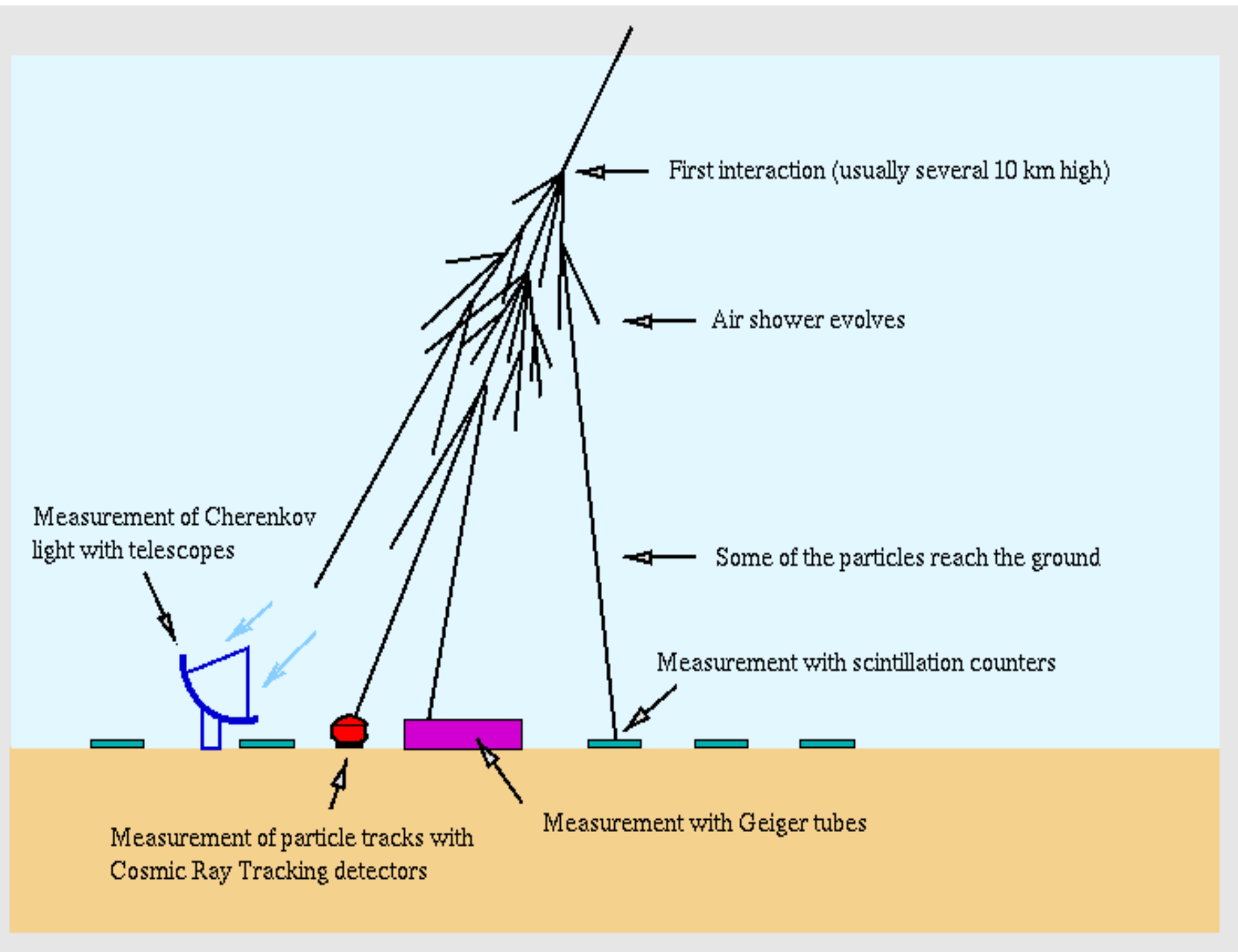
Maximum rigidity(MDR) $=400 \text{ GeV/c}$ weight $=400 \text{ kg}$. Electrical consumption $=300 \text{ W}$



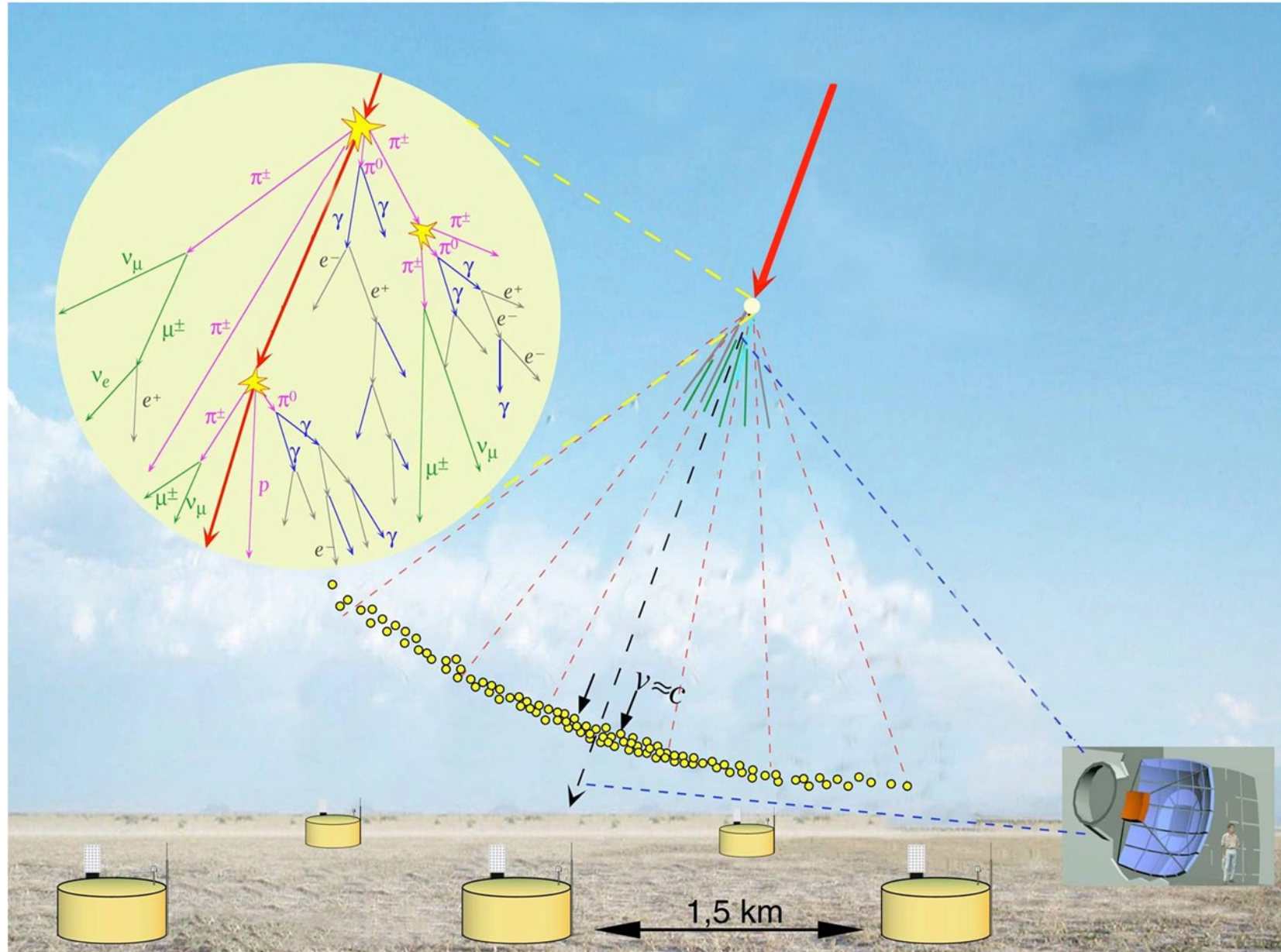


AMS 02

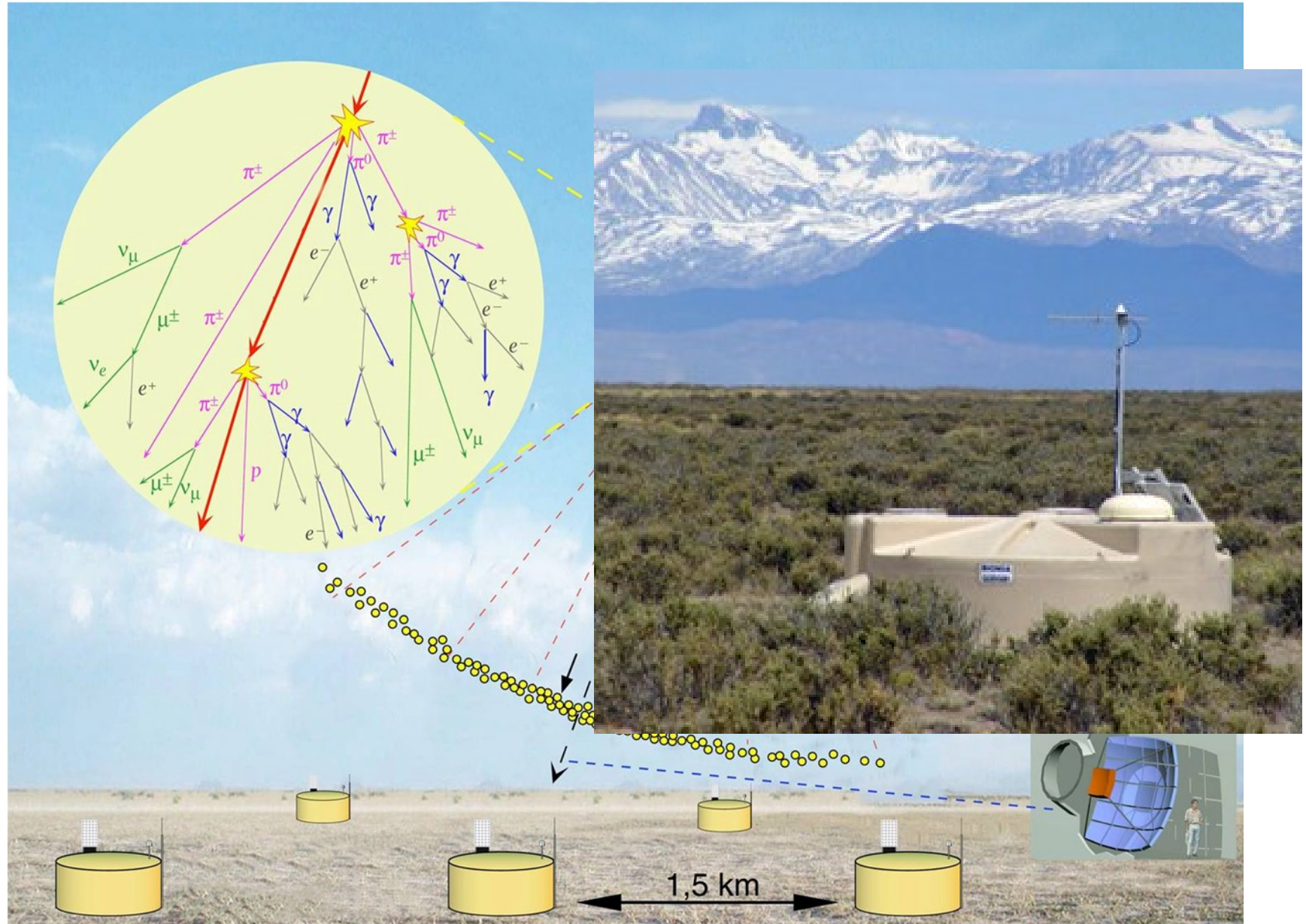




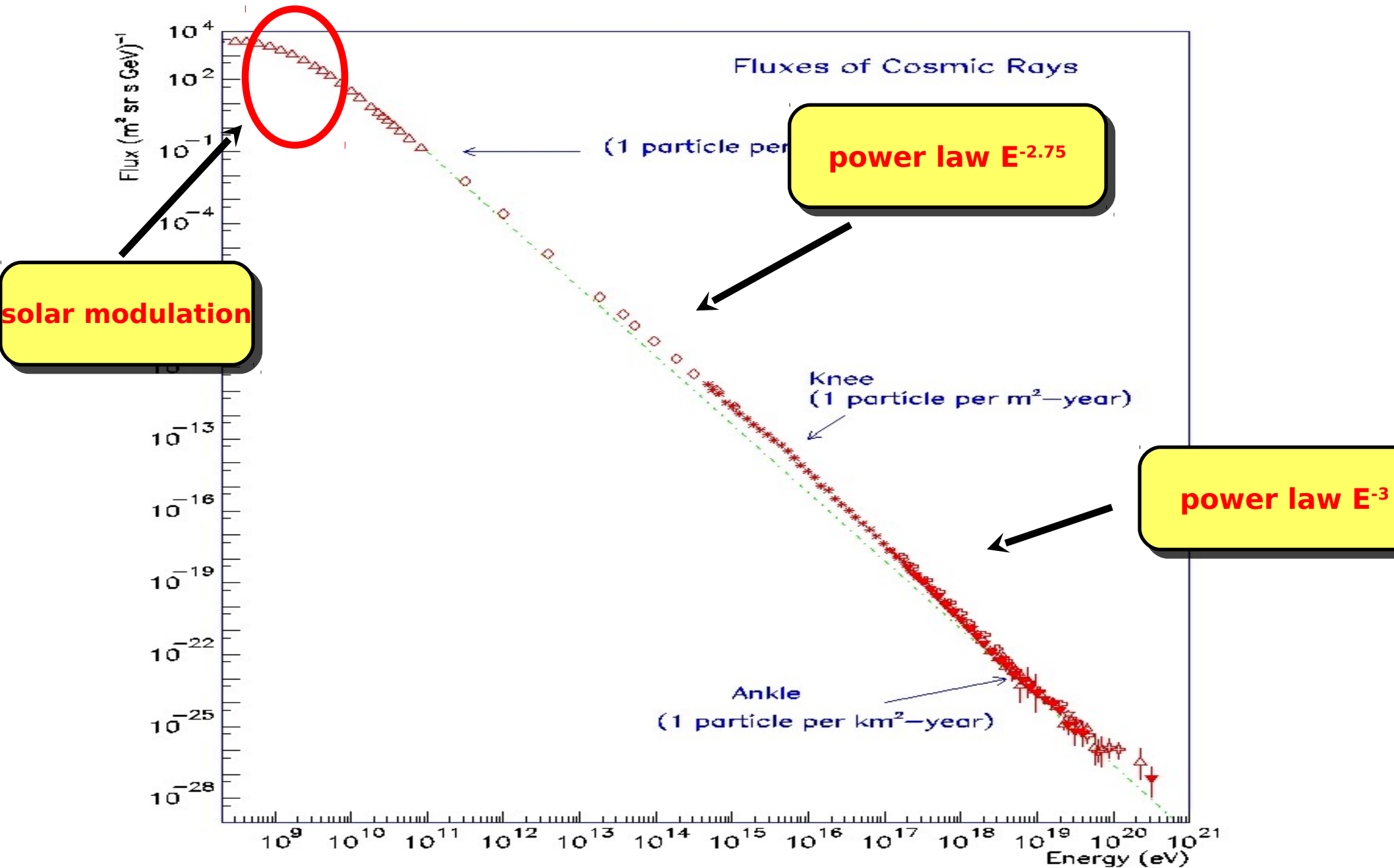
Auger Observatory

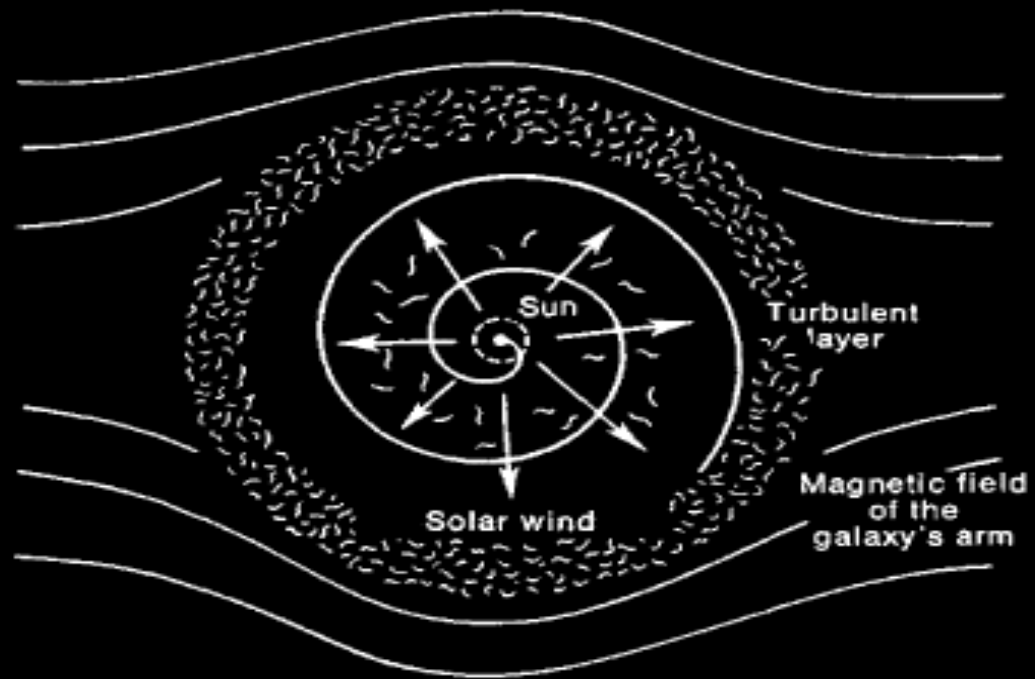


Auger Observatory

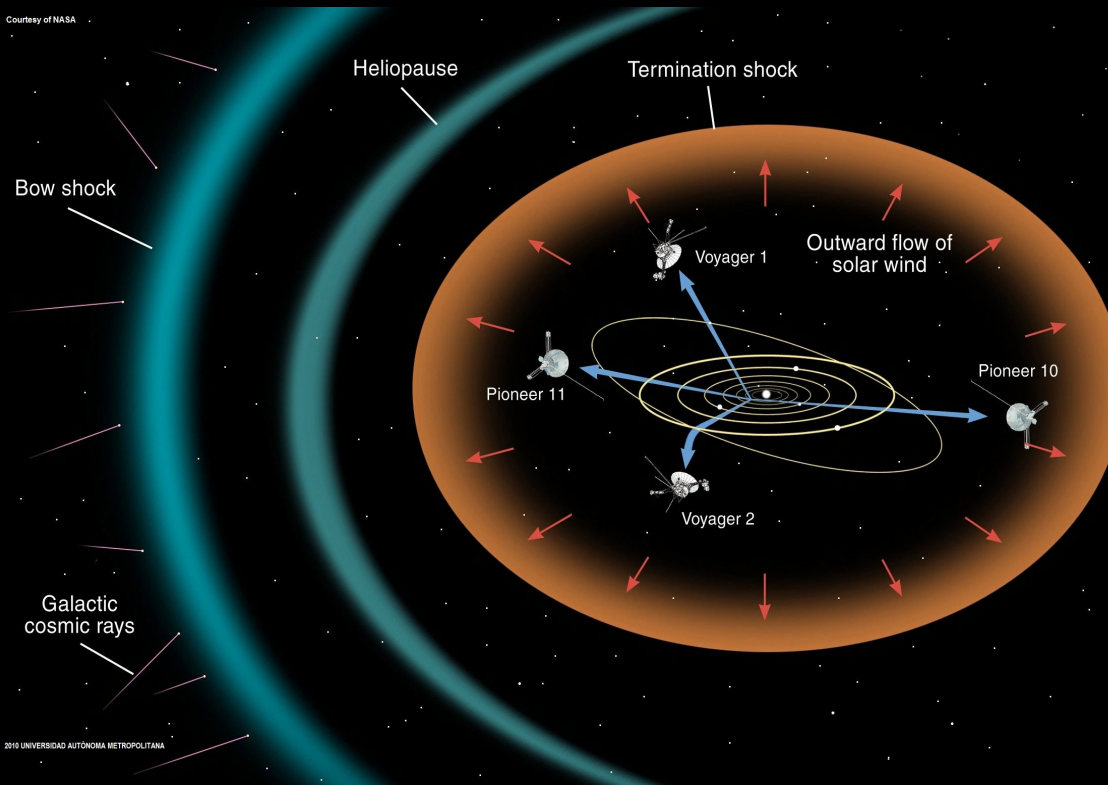


The (local) Cosmic Ray spectrum

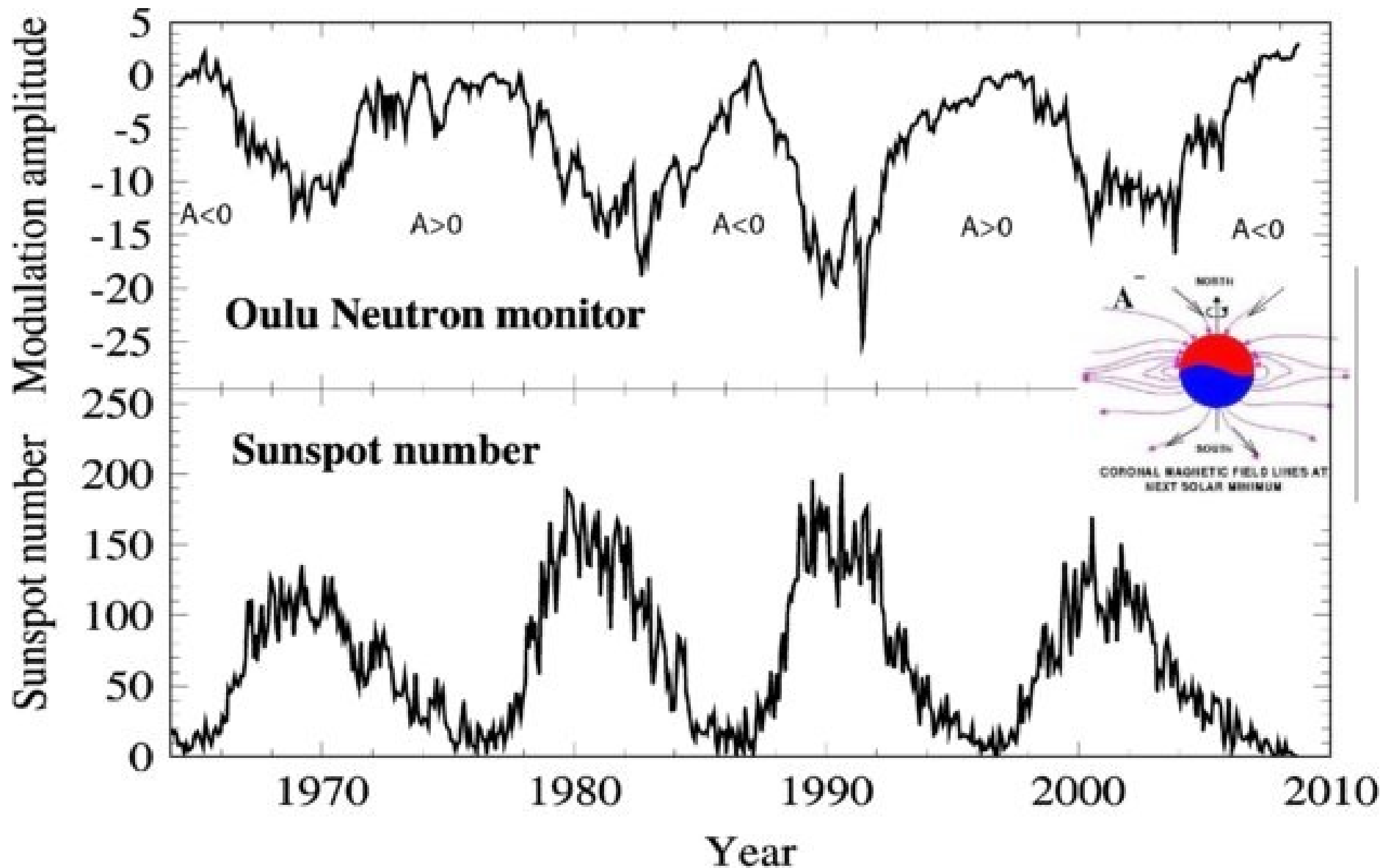




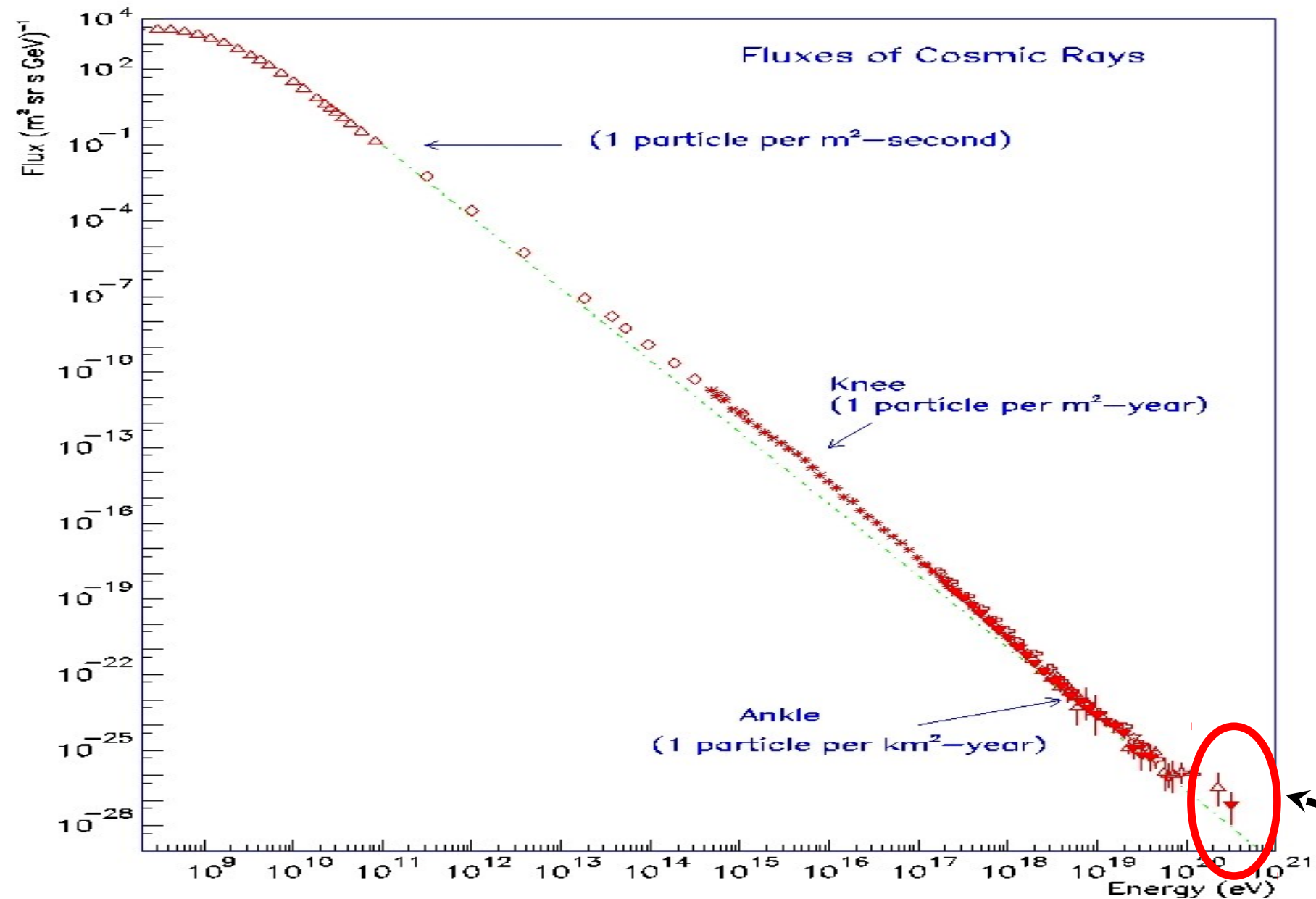
Courtesy of NASA



Solar modulation

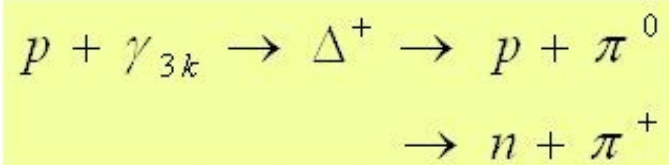


The (local) Cosmic Ray spectrum



GKZ suppression

- Cosmic rays $E = 10^{20}$ eV interact with 2.7 K photons
- In the proton frame $E_\gamma = 300$ MeV



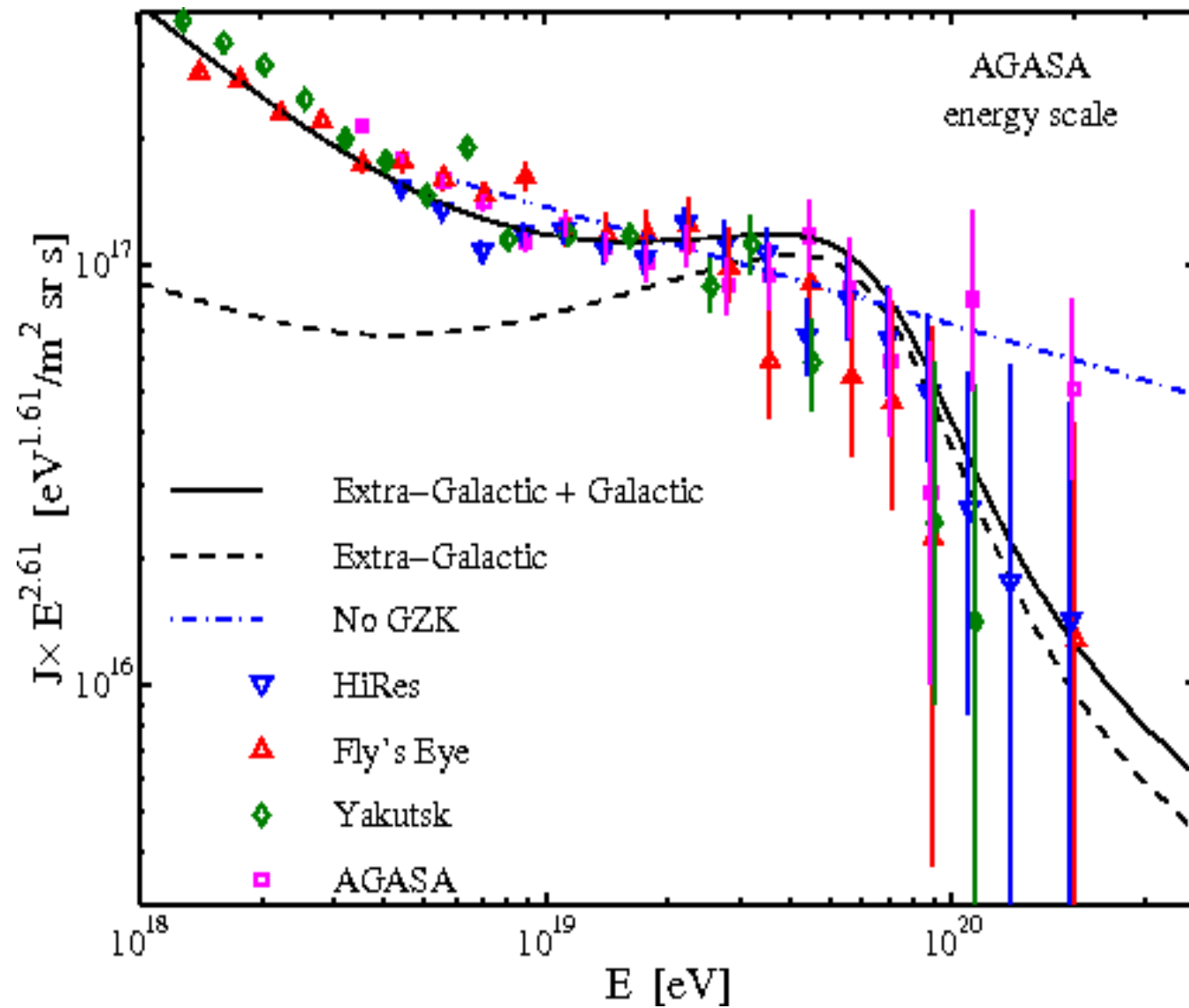
Photon-pion production

Photon dissociation

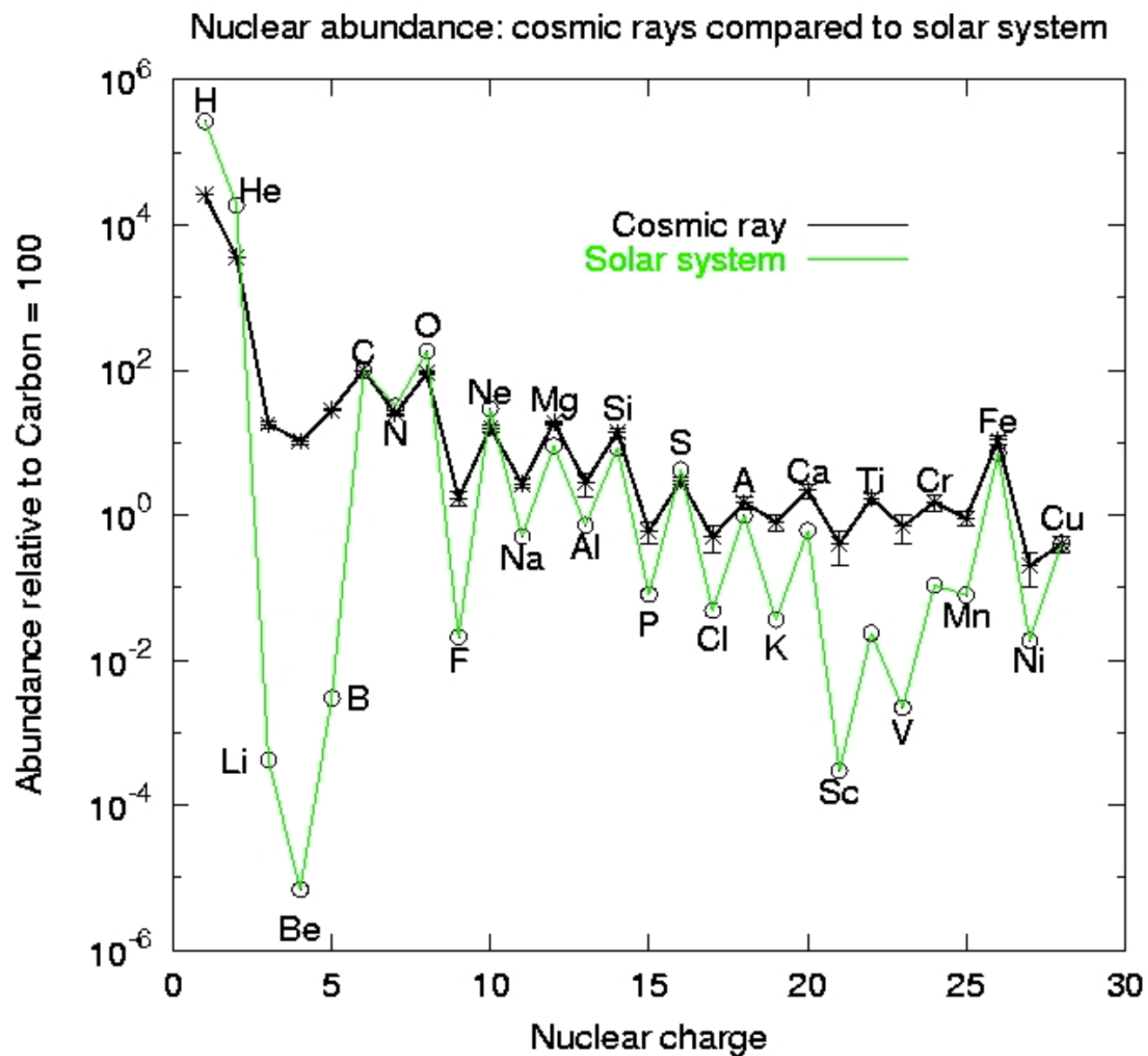
- Nuclei
- Proton with less energy, eventually below the cutoff energy
 $E_{\text{GZK}} = 5 \times 10^{19}$ eV

Universe is opaque for $E > E_{\text{GZK}}$!

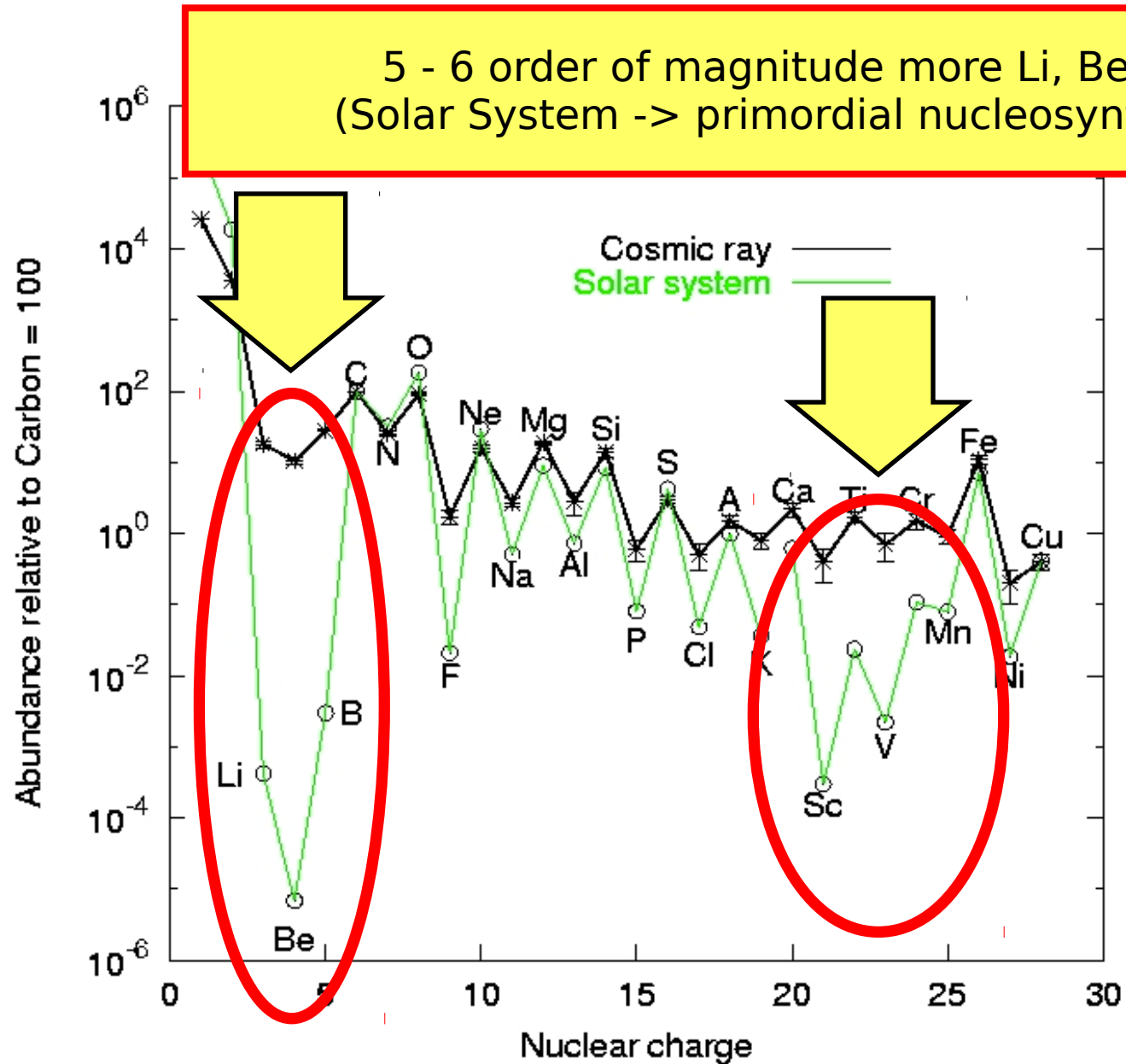
GZK Effect



Cosmic Ray composition



Cosmic Ray composition

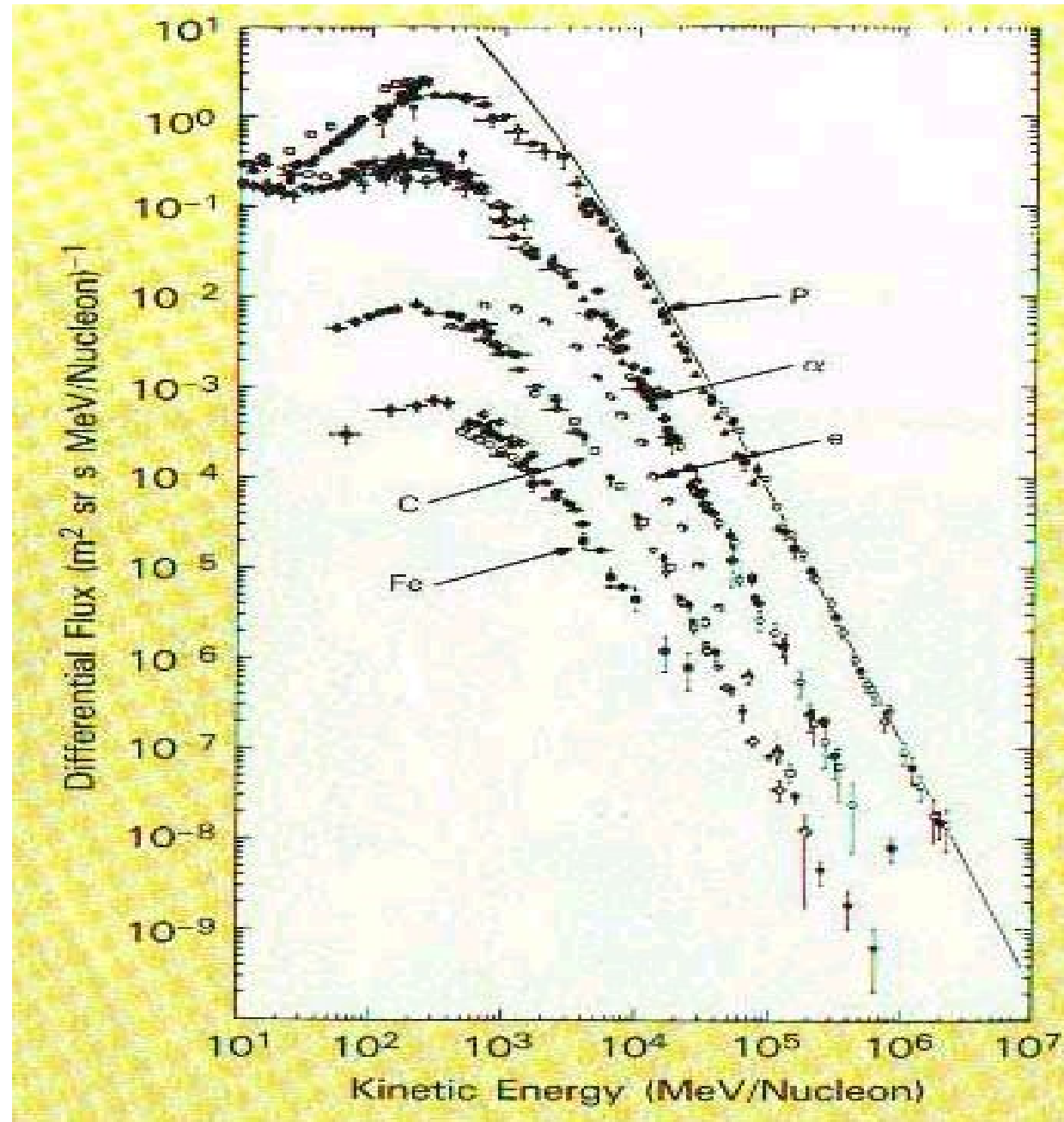


The chemical composition

All energy distributions have power-law shapes at high energies, with very similar slopes for the different species.

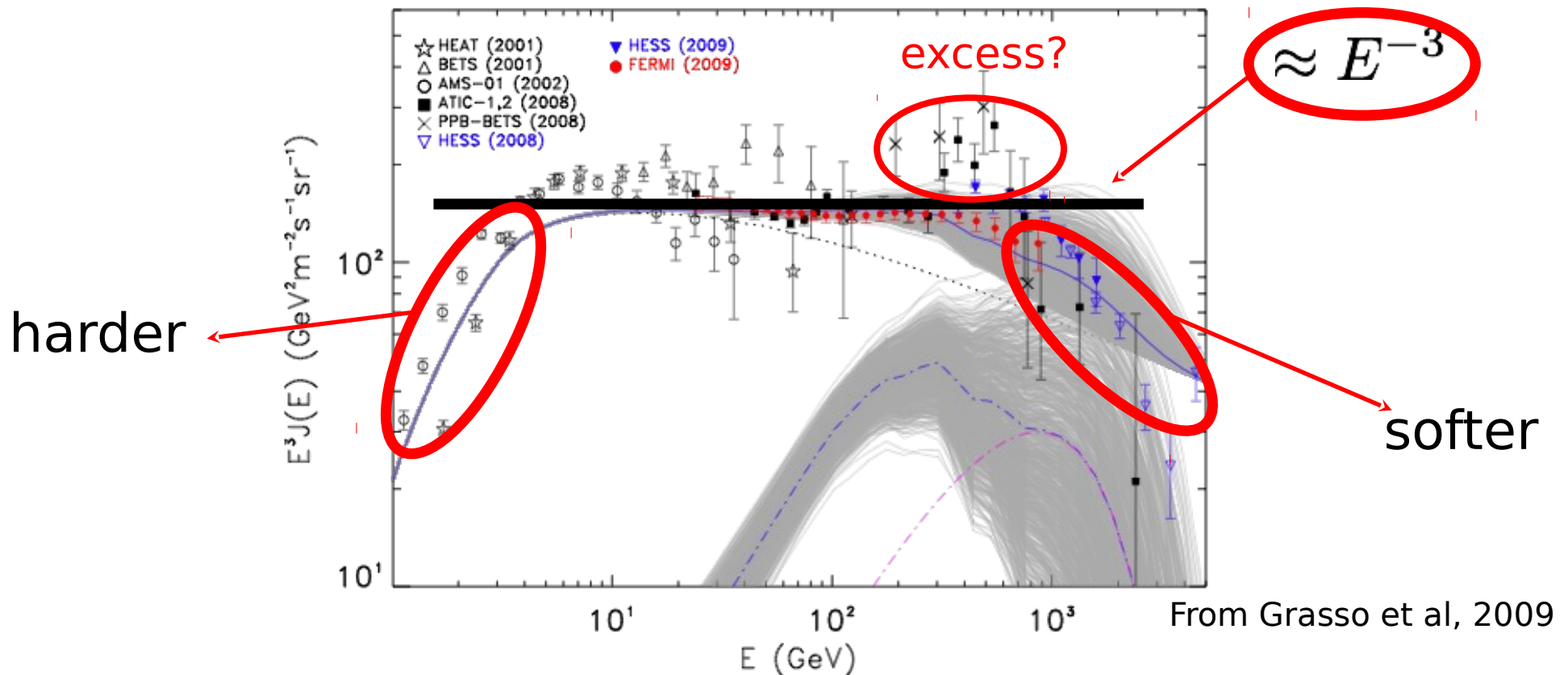
The form of these spectra provides important clues to the mechanism of acceleration.

Subtle differences among these spectra provide information transport processes by which cosmic rays propagate through the Milky Way to arrive at the Earth.



Cosmic Ray electrons

The CR electron spectrum is more structured (and more difficult to be measured) of the proton one



@ ~1 GeV --> $N_p/N_e \sim 100$

Cosmic Ray electrons

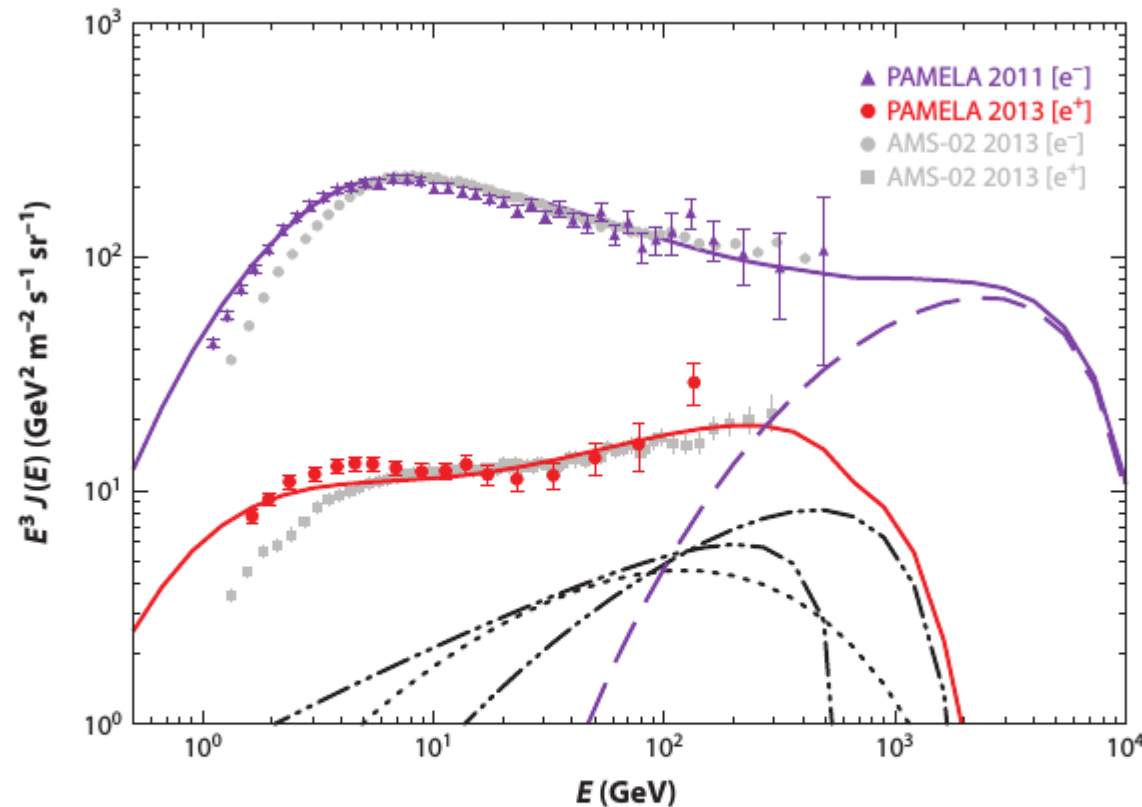
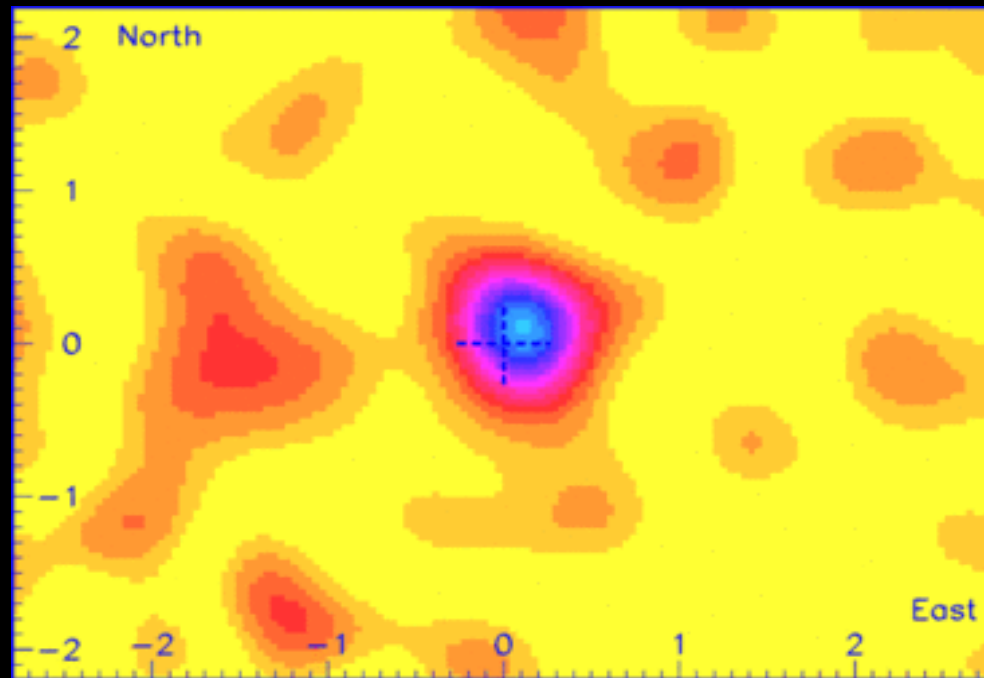


Figure 2

Cosmic-ray electron and positron spectra from AMS-02 and PAMELA compared with 3D models with possible contributions from nearby pulsars (*long dashed line* for Vela, *double dotted-dashed lines* for Monogem and Geminga) and an additional component (*dotted line*) required to explain the data (from Gaggero et al. 2014). Solid lines show the total spectra including the Galactic primary and secondary leptons. Solar modulation is modelled to a level appropriate to the PAMELA data. Adapted with permission from Gaggero et al. 2014. Copyright by the American Physical Society.

Arrival direction



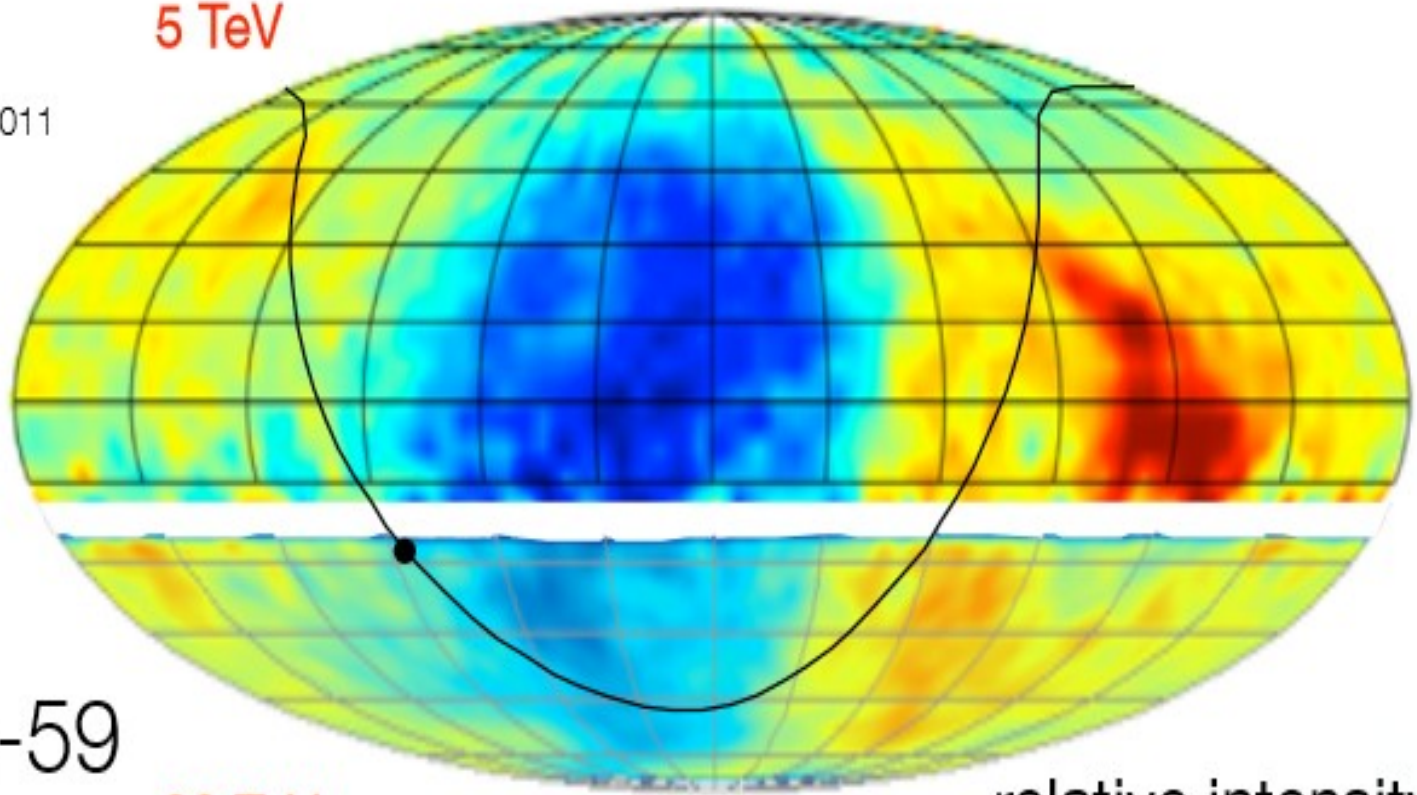
The Moon's cosmic ray shadow, as seen in secondary muons detected 700 m below ground, at the Soudan 2 detector

CR Anisotropy

Tibet-III

Amenomori et al., ICRC 2011

5 TeV

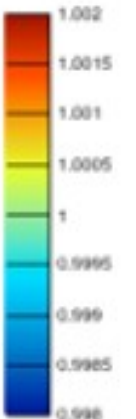
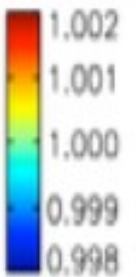


IceCube-59

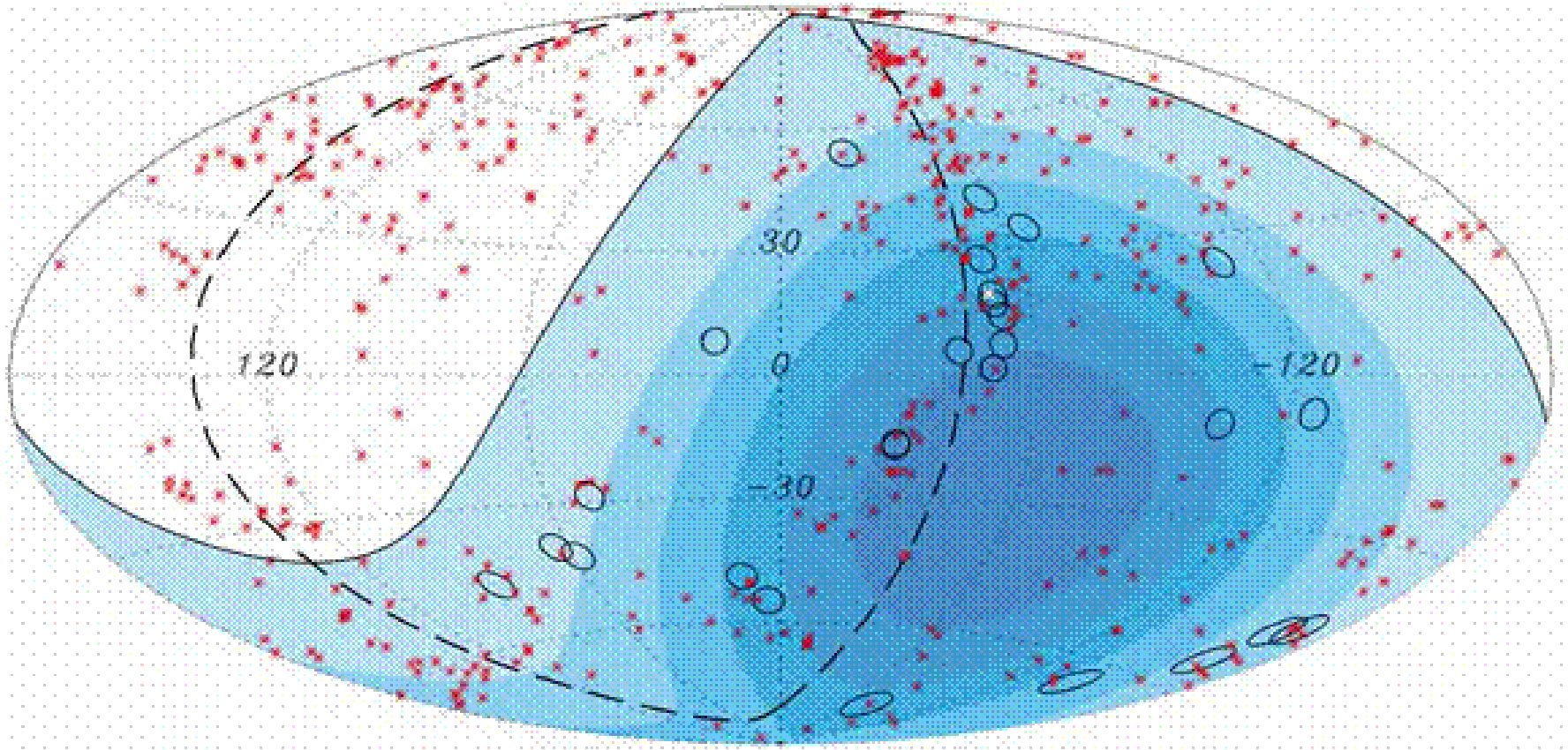
Abbasi et al., ApJ, **746**, 33, 2012

20 TeV

relative intensity



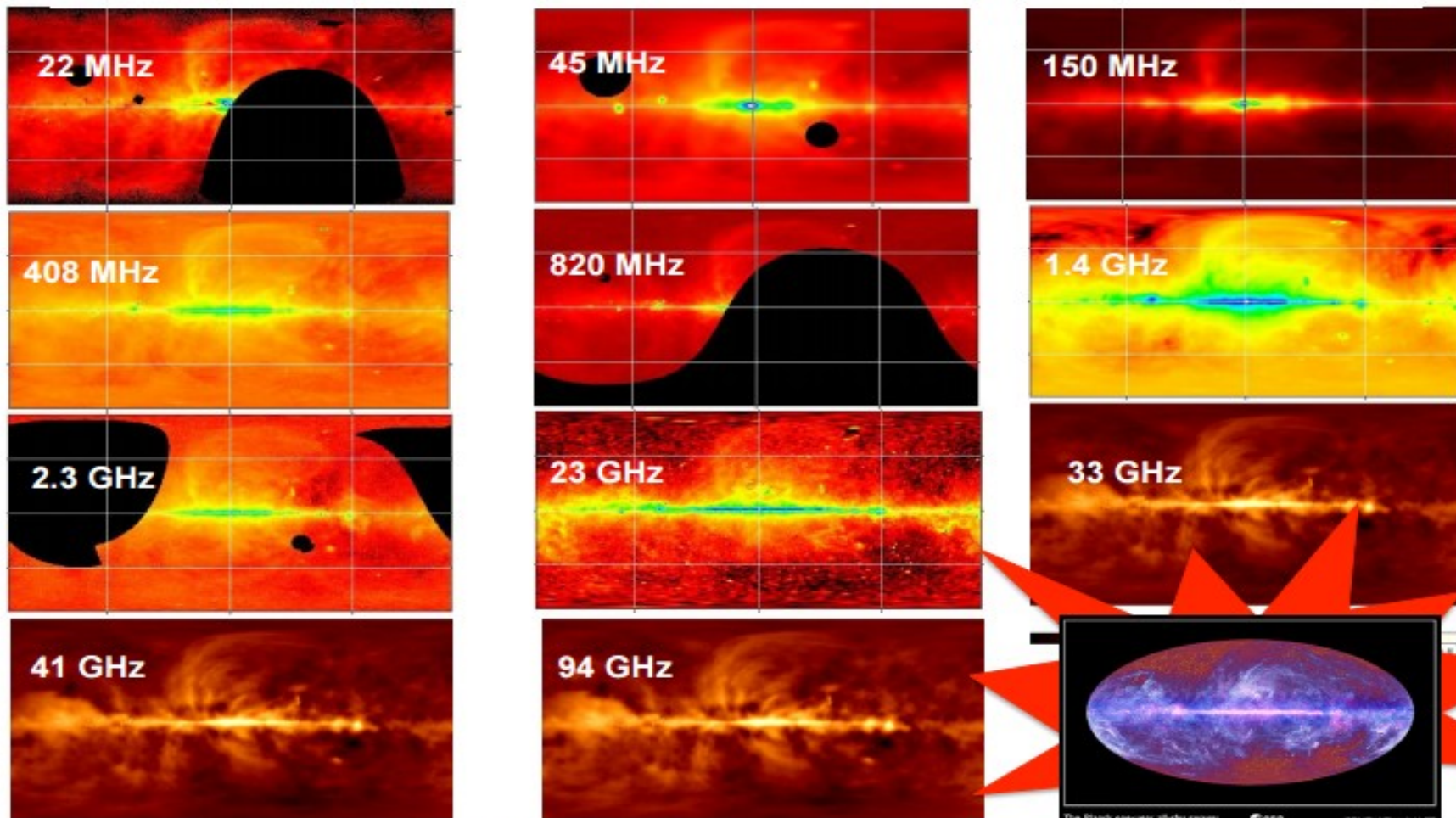
UHE CR



Arrival directions of incoming cosmic rays as measured at the Pierre Auger Observatory (black circles) and positions of known active galactic nuclei (red dots) up to the distance of 75 Megaparsecs

Radio emission of the Galaxy

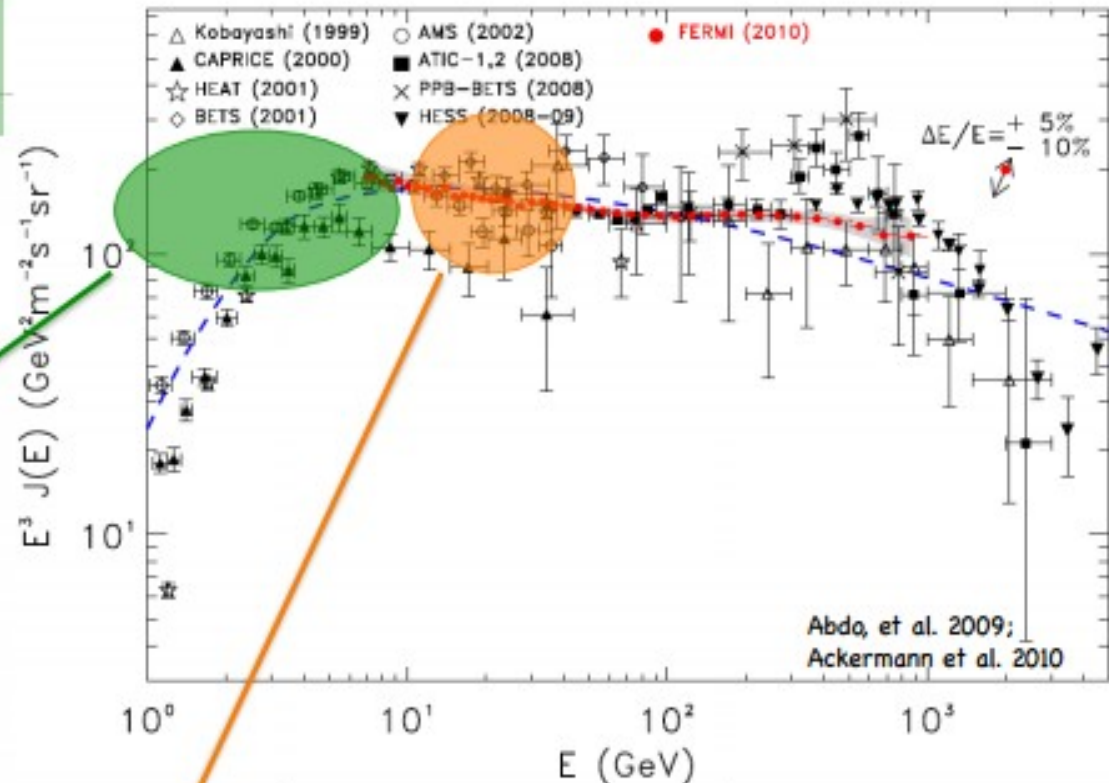
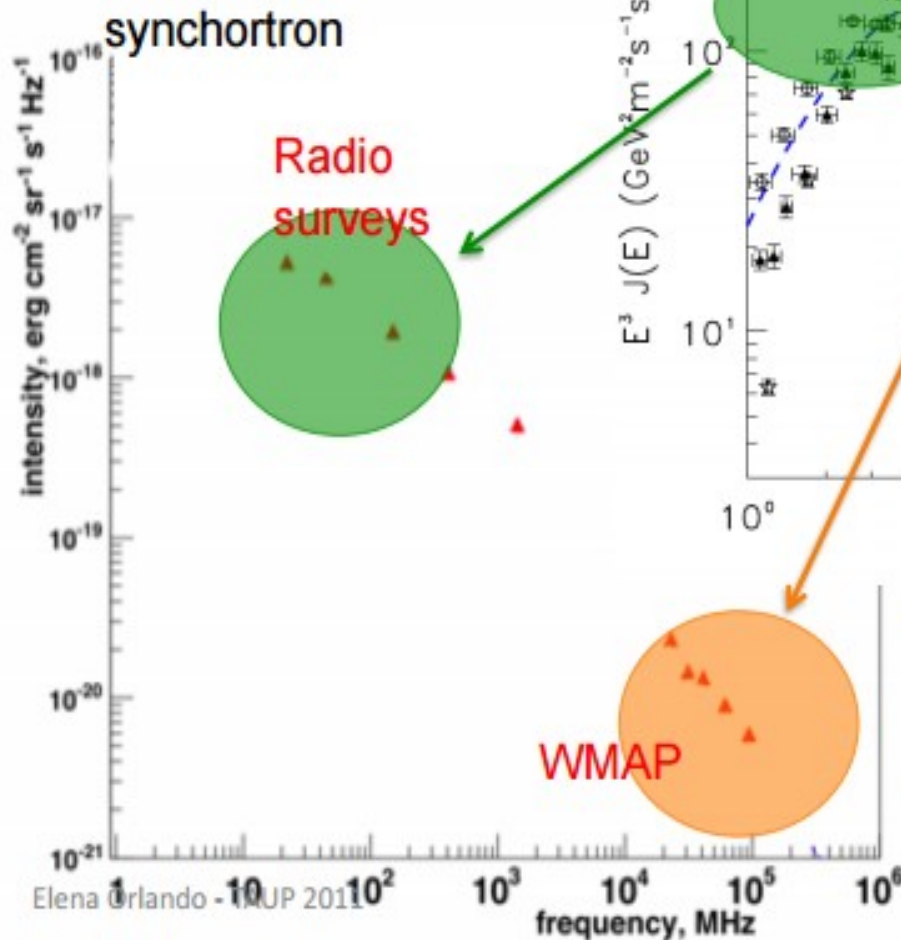
Radio surveys & WMAP



Radio Ground-based Surveys: 22 MHz – 5 GHz
WMAP: 23 – 94 GHz Planck: 30 – 800 GHz

Radio emission of the Galaxy

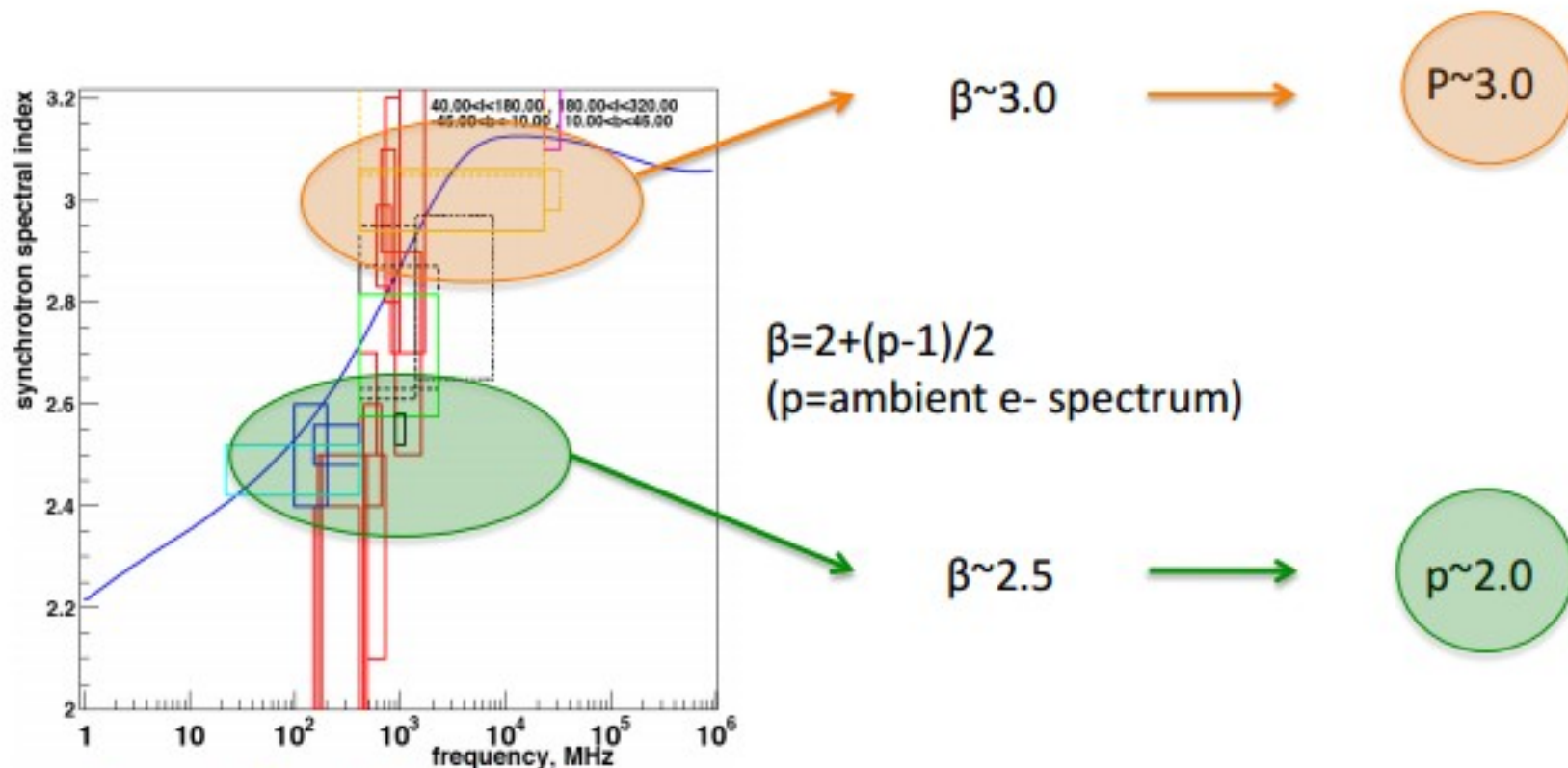
Probe of interstellar spectrum before modulation



Probe of interstellar spectrum directly measured. Good determination of B field

Radio emission of the Galaxy

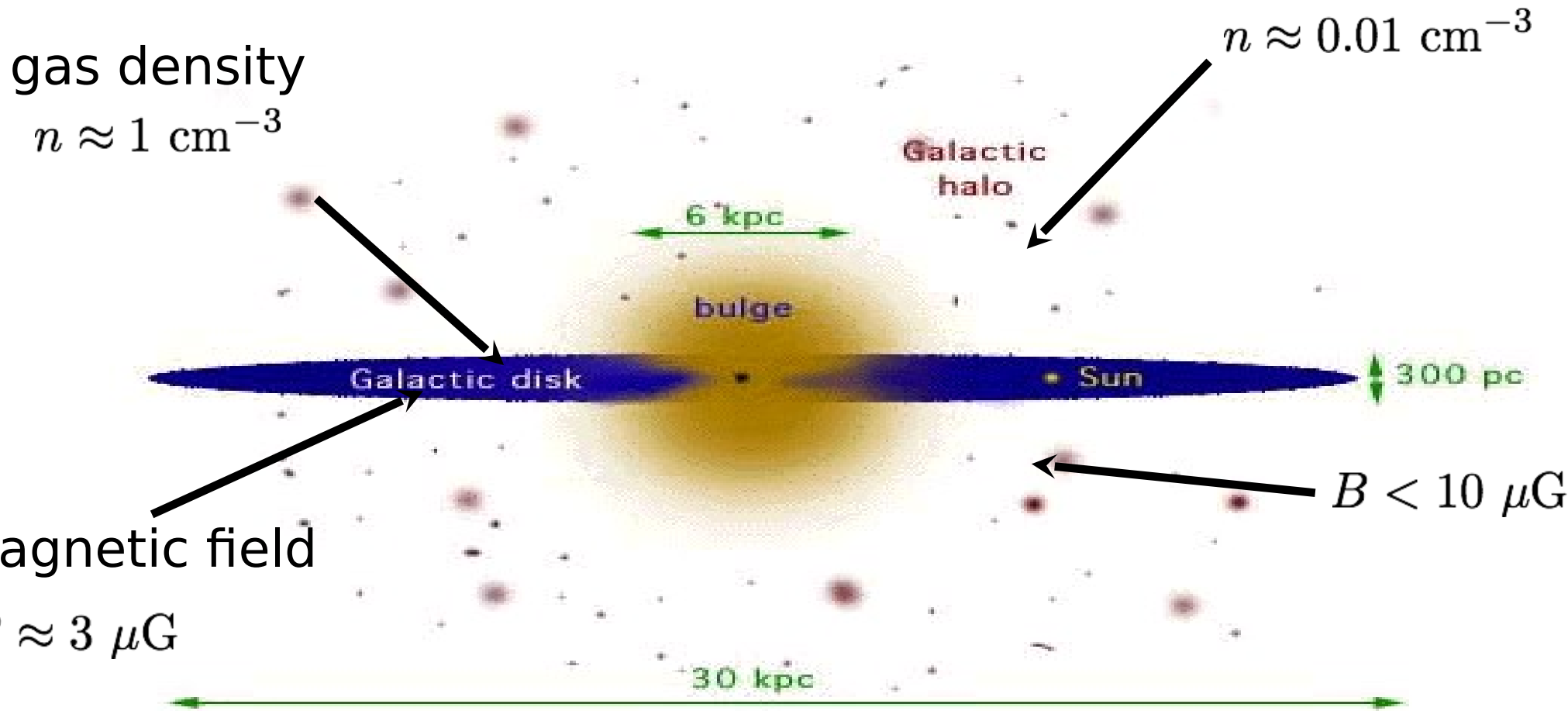
Synchrotron spectral index measurements ...



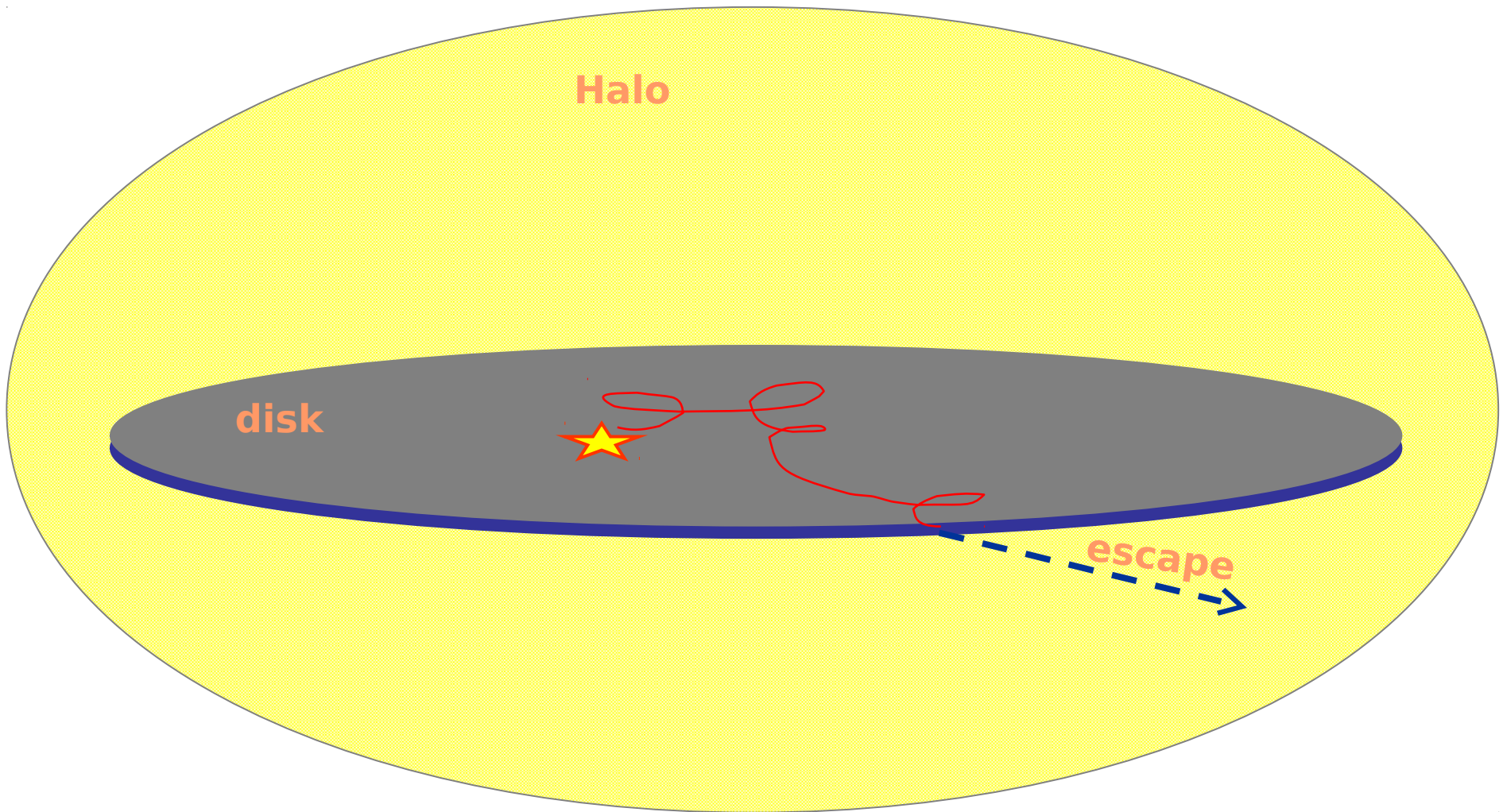
Strong, Orlando & Jaffe A&A
accepted (arXiv:1108.4822)

... need of a break in interstellar e-

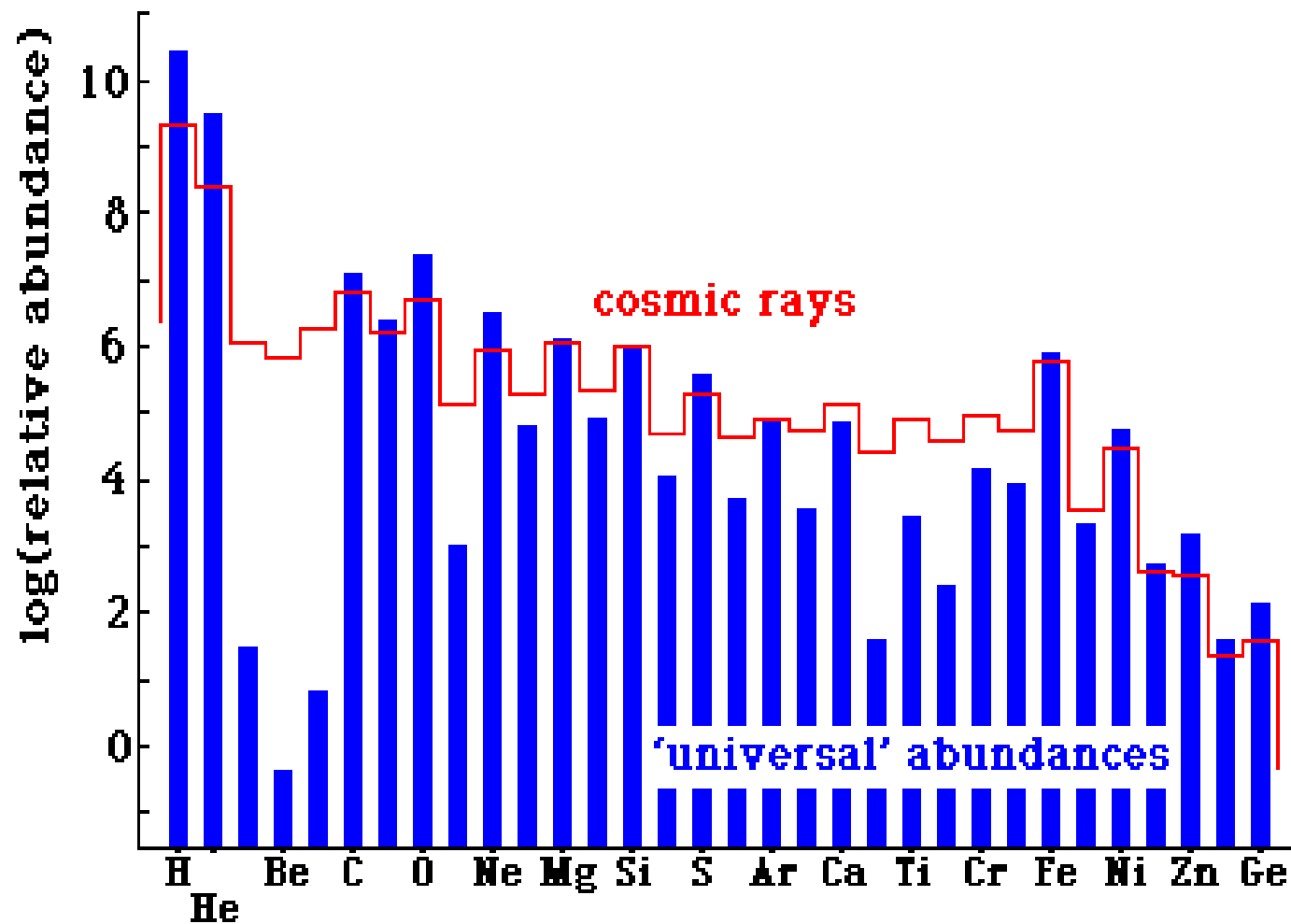
the Milky Way



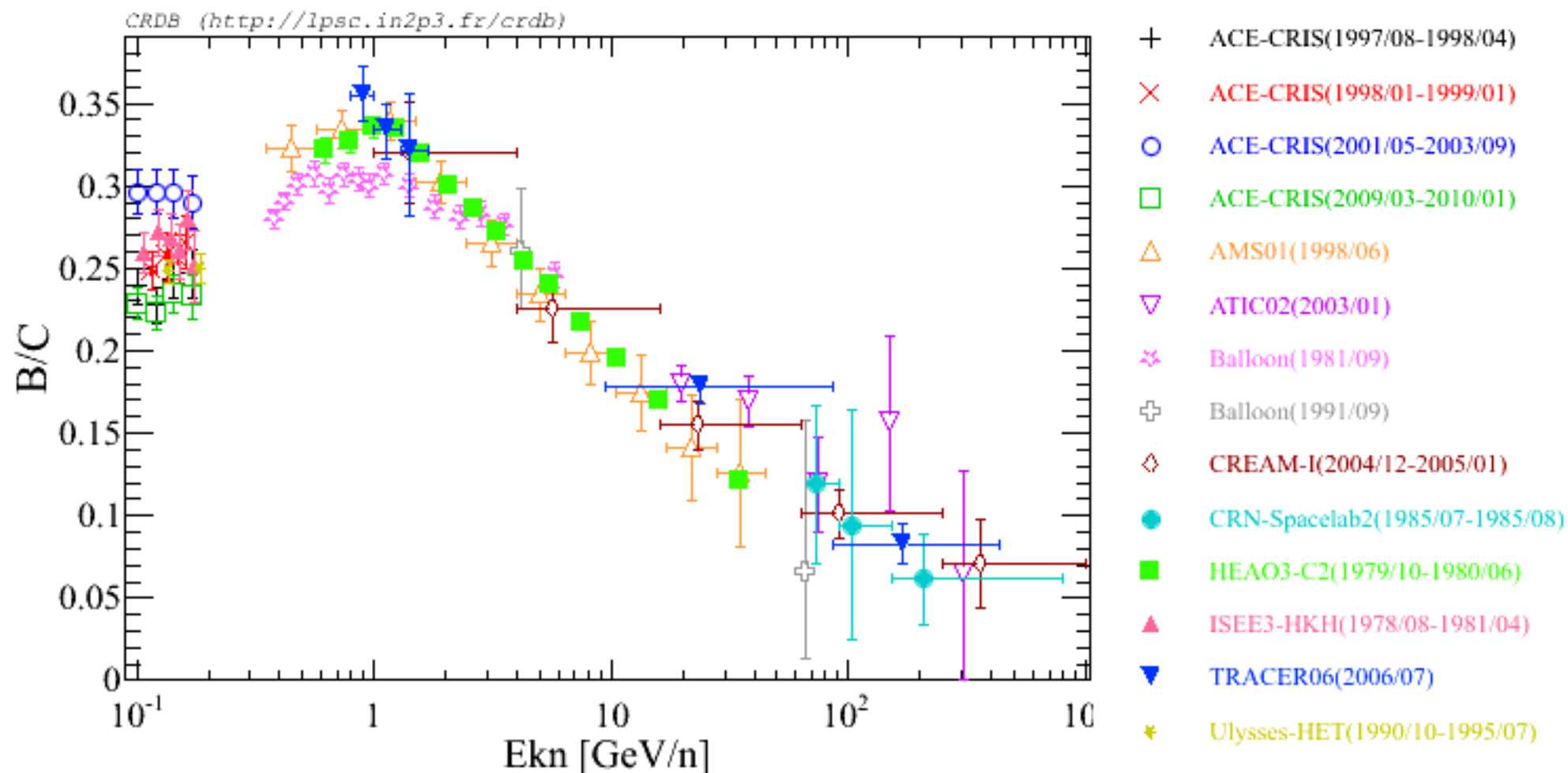
CR Propagation



Nuclei Spallation



B/C Ratio

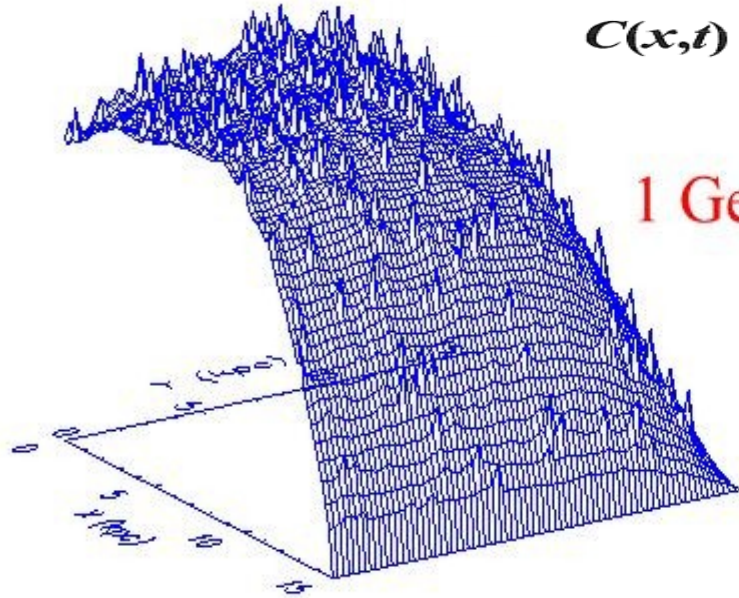


particle #0 electrons:1.02e+03 MeV

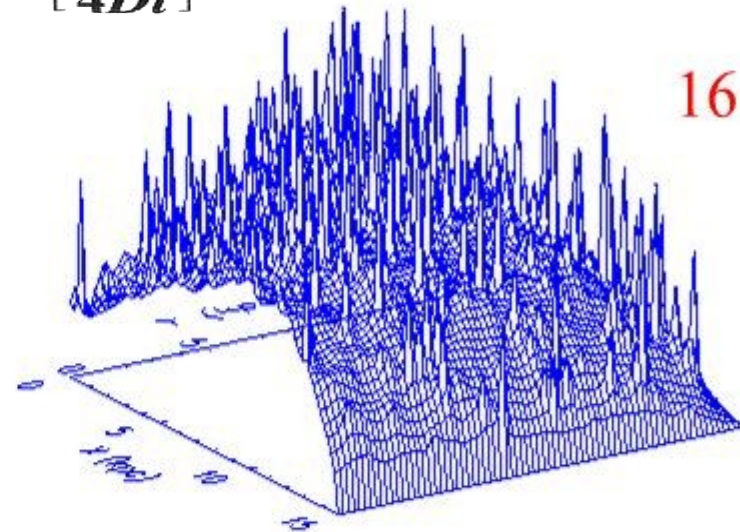
particle #0 electrons:1.64e+04 MeV

$$C(x,t) = \frac{S}{\sqrt{\pi Dt}} \exp\left[\frac{-x^2}{4Dt}\right]$$

1 GeV



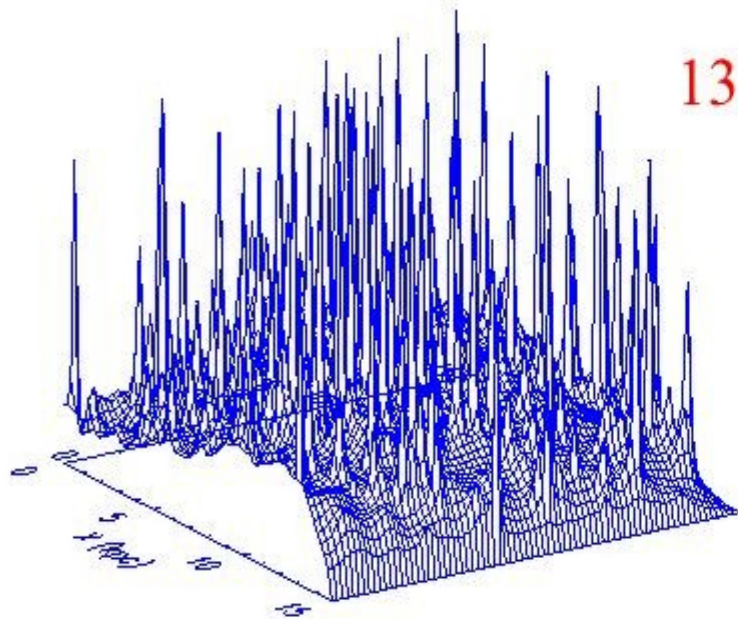
16 GeV



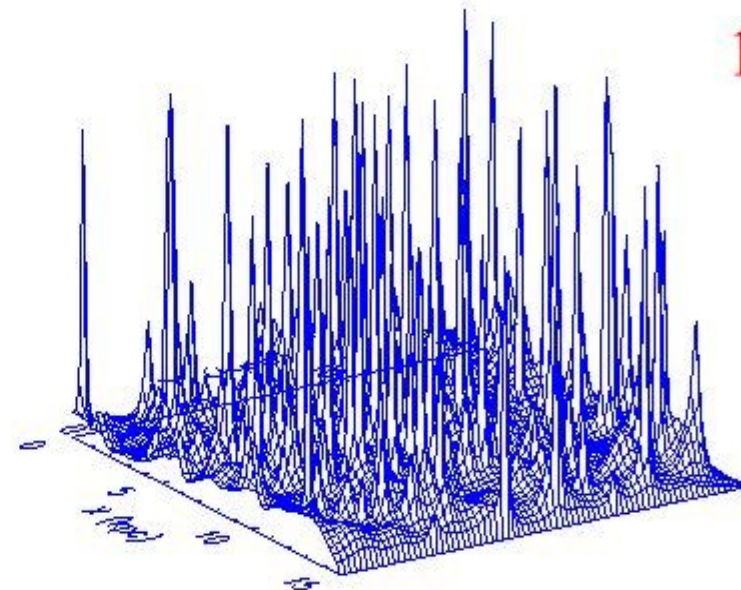
particle #0 electrons:1.31e+05 MeV

particle #0 electrons:1.05e+06 MeV

130 GeV



1 TeV



Diffusion of CR in the ISM

$$\frac{dn(E, r)}{dt} = D(E) \nabla^2 n(E, r) - \frac{\partial}{\partial E} n(E, r) b(E) + Q(E, r)$$



Diff. in physical space



Energy losses



Source

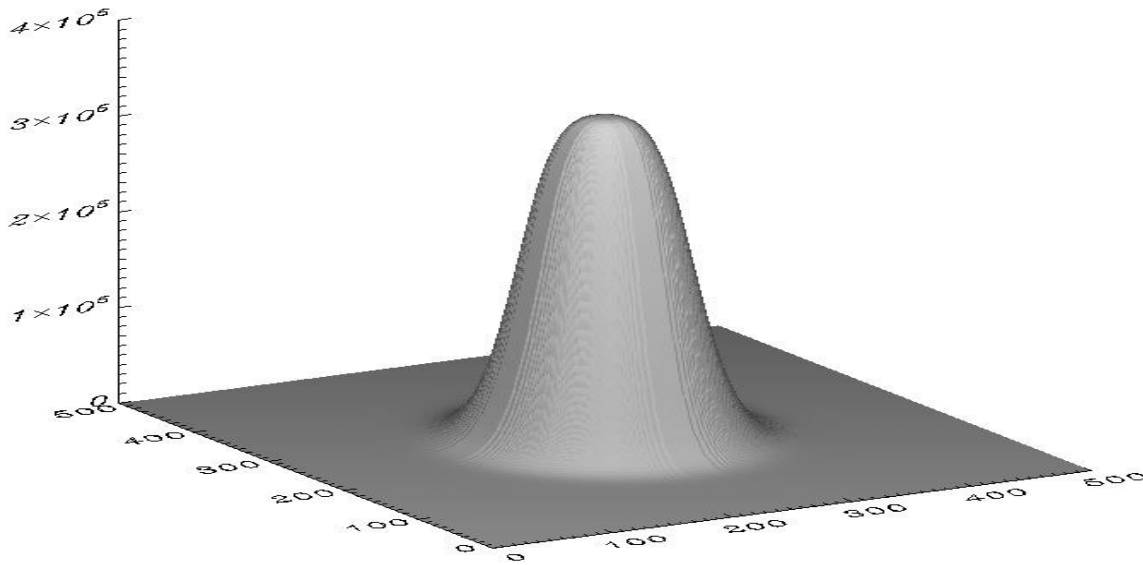
Diffusion of CR in the ISM

$$\frac{dn(E, r)}{dt} = D(E) \nabla^2 n(E, r) - \cancel{\frac{\partial}{\partial E} n(E, r) b(E)} + \cancel{Q(E, r)}$$

For an impulsive source
and ignoring E losses :

$$n(E, r) = \frac{S}{\sqrt{\pi D t}} \exp\left[\frac{-x^2}{4 D t}\right]$$

$$R_{diff}(E, t) = 2\sqrt{D(E)t}$$



Extended gamma-ray sources around pulsars constrain the origin of the positron flux at Earth

A. U. Abeysekara¹, A. Albert², R. Alfaro³, C. Alvarez⁴, J. D. Álvarez⁵, R. Arceo⁴, J. C. Arteaga-Velázquez⁵, D. Avila Rojas³, H...

✚ See all authors and affiliations

Science 17 Nov 2017;
Vol. 358, Issue 6365, pp. 911-914
DOI: 10.1126/science.aan4880

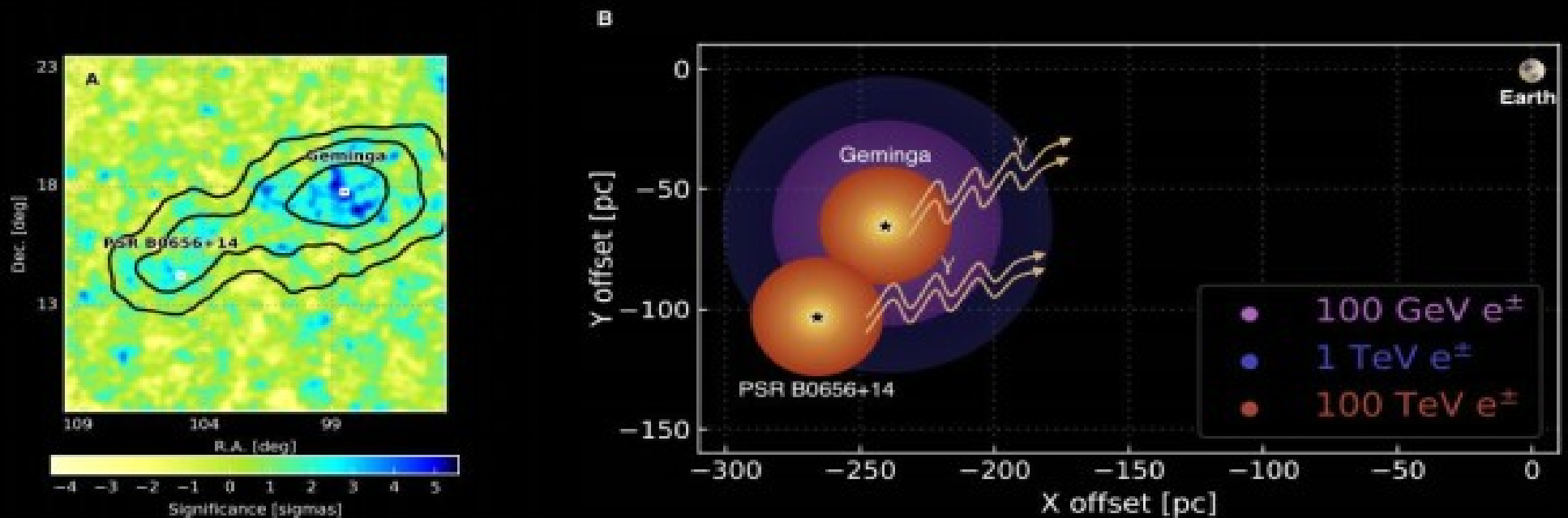


Fig. 1: Spatial Morphology of Geminga and PSR B0656+14. (A) HAWC significance map (between 1 and 50 TeV) for the region around Geminga and PSR B0656+14, convolved with the HAWC point spread function and with contours of 5σ , 7σ , and 10σ for a fit to the diffusion model. R.A., right ascension; dec., declination (B) Schematic illustration of the observed region and Earth, shown projected onto the Galactic plane. The colored circles correspond to the diffusion distance of leptons with three different energies from Geminga; for clarity, only the highest energy (blue) is shown for PSR B0656+14. The balance between diffusion rate and cooling effects means that tera-electron volt particles diffuse the farthest (Fig. S1).